EFFECT OF OSCILLATOR INSTABILITY ON TELEMETRY SIGNALS

by Terry L. Grant *and* Randolph L. Cramer

Ames Research Center
Moffett Field, Calif. 94035

1. Report No. NASA TN D-6442	2. Government Accession No.	3. Reci,

4. Title and Subtitle	5. Report Date
EFFECT OF OSCILLATOR INSTABILITY ON TELEMETRY SIGNALS	July 1971
	6. Performing Organization Code

7. Author(s)	8. Performing Organization Report No.
Terry L. Grant and Randolph L. Cramer	A-3836

	10. Work Unit No.
	125-21-10-02-00-21

9. Performing Organization Name and Address	
NASA Ames Research Center Moffett Field, Calif. 94035	11. Contract or Grant No.

	13. Type of Report and Period Covered
12. Sponsoring Agency Name and Address	Technical Note
National Aeronautics and Space Administration Washington, D. C. 20546	14. Sponsoring Agency Code

15. Supplementary Notes

16. Abstract

This paper discusses short-term oscillator instability and its effect on telemetry signals. Instability measurements are related to the total phase jitter expected in a telemetry receiver and the resulting degradation of telemetry performance. The analysis of phase jitter present in the telemetry system of Pioneer VI through IX serves as an example. The instability is described by the measurement of oscillator phase jitter, and the function and operation of the measuring instrument are explained.

17. Key Words (Suggested by Author(s))	18. Distribution Statement
Oscillator Instability Pioneer Spacecraft Short Term Phase Modulation Phase Jitter Error Rate Phase Noise Time Average of Random Characterization Process Telemetry Receiver	Unclassified – Unlimited

19. Security Classif. (of this report)	20. Security Classif. (of this page)	21. No. of Pages	22. Price*
Unclassified	Unclassified	41	$3.00

TABLE OF CONTENTS

SYMBOLS

A,B,C,D   amplitude terms in the polynomial representing the power spectral density of phase jitter

B_L equivalent noise power bandwidth of a phase lock loop

e_o modulated signal plus additive noise

e_p output of the telemetry phase detector

e_{PL} low pass filtered telemetry phase detector output

f_c carrier frequency, Hz

$F(j\omega)$ transfer function for the linear model of the loop filter in a phase lock loop, PLL

G   peak amplitude of a telemetry signal

g(x)   probability density function for $\cos \phi(t)$

$H(j\omega)$ transfer function for the linear model of a phase lock loop

h(x)   probability density function for $\frac{1}{TK} \int_o^T n(t)\, dt$, a gaussian density

I_o zeroth-order modified Bessel function

K   modulation constant proportional to the modulation index for the telemetry

K_D transfer constant for the linear model of a phase detector

$\frac{K}{j\omega}$ integration transfer function for the linear model of a voltage controlled oscillator

M(t)   modulating signal on the telemetry carrier

$n_i(t)$ in-phase component of additive noise

$n_q(t)$ quadrature component of additive noise

n(t)   additive noise on the modulation

P_e probability of an error in the telemetry symbols

$p_q(x)$ combined probability density function, formed from g(x) and h(x) by convolution

$p(\phi)$ probability density function of phase jitter

q	normalized decision variable
q_K	decision variable
$S_\phi(\omega)$	power spectral density of phase jitter
T	symbol period
T_c	carrier period, $\left(\dfrac{1}{f_c}\right)$
t	time
$\overline{U_{in}^2}$	mean square value of the upper bound approximation for ϕ_{in}
U_{RMS}	$\sqrt{\overline{U_{in}^2}}$, the root mean square value of U_{in}
α	reciprocal of the variance of phase jitter
Δt	time increment
$\Delta\phi$	phase increment
δ	damping factor of a phase lock loop
σ_ϕ^2	variance of phase jitter
τ_1, τ_2	time constants for $F(j\omega)$
$\overline{\phi^2}$	mean square value of ϕ
ϕ_{in}	phase jitter internal to a signal
ϕ_{RMS}	$\sqrt{\overline{\phi_{in}^2}}$, the root mean square value of ϕ_{in}
$\phi(t)$	phase jitter, one realization of the random process
ϕ_x	phase jitter external to a signal and proportional to the noise-to-signal ratio
ω	frequency, rad/s
ω_c	carrier frequency, rad/s
ω_{if}	half the bandwidth of a receiver intermediate frequency amplifier, rad/s
ω_n	natural frequency of a phase lock loop, rad/s

EFFECT OF OSCILLATOR INSTABILITY ON TELEMETRY SIGNALS

Terry L. Grant and Randolph L. Cramer

Ames Research Center

SUMMARY

This paper discusses short-term oscillator instability and its effect on telemetry signals. Instability measurements are related to the total phase jitter expected in a telemetry receiver and the resulting degradation of telemetry performance. The analysis of phase jitter present in the telemetry system of Pioneer VI through IX serves as an example. The instability is described by the measurement of oscillator phase jitter, and the function and operation of the measuring instrument are explained.

INTRODUCTION

In spacecraft telemetry the trend has been to use a pulse code modulation - phase shift keyed - phase modulated (PCM-PSK-PM) system because, with coherent carrier detection, such a system can theoretically provide the lowest error rate for a given signal-to-noise ratio of all the known modulation techniques. The key factor in obtaining this performance, however, is the coherent or phase-tracking detection process, and deviation from this ideal model quickly causes a loss of performance. It was the quest to make the Pioneer telemetry system perform as well as possible which motivated the measurement of oscillator instability and the analysis of its effect on a telemetry system. (Performance here is understood as the channel error rate versus a normalized signal-to-noise ratio.) Lack of coherence in carrier tracking also affects the resolution of any range and range rate measurements that may be made on the telemetry carrier.

In the design of an optimum coherent, or phase-tracking telemetry system, several sources of phase jitter must be considered. The most obvious source is the additive noise in the bandwidth of the tracking loop. A second source of phase jitter is oscillator instability in the transmitter reference oscillator or the receiver voltage controlled oscillator (VCO). Other sources are propagation anomalies that affect the phase of the carrier. The latter are caused by small time varying changes in the dielectric medium (ref. 1). Only oscillator instability as a source of phase jitter will be treated here and its effects on the performance of a one-way (spacecraft-to-ground) telemetry system will be analyzed. It then will be shown how this source of phase jitter forms an important bound on telemetry performance.

This paper is a tutorial description of oscillator instability and its effects on a phase lock loop (PLL). Measured phase jitter is used to analyze statistically the conditions under which this jitter will degrade the performance of a one-way (spacecraft-to-ground) telemetry system. The appendixes discuss the concepts of probability and statistics which are key to the analysis. Finally, the oscillator instability measuring instrument is described and the results of measurements on the oscillator circuits of the Pioneer transmitter are presented. These data formed the basis for the assumptions of the character of oscillator instability. (The Pioneer telemetry system provided the example that motivated the analysis of the effect of oscillator instability on a telemetry system.)

ANALYSIS

The key factor in obtaining optimum performance with a PSK communication system is maintaining a coherent reference to compare with the transmitted signal. Although theoretically no signal power is allowed for this reference, it is necessary in practice. Theoretically, both the transmitter and the receiver have perfect time information available; therefore nothing would be gained by including a time reference with the signal. In reality, sufficiently accurate time information is not available to allow coherent phase detection. The following example illustrates this point. Suppose the clocks at a transmitter and receiver measure time to a relative accuracy of ±1 μs (a difficult feat within the present state of the art). Suppose further that the known signal is PSK modulated of the form, $\sin[\omega_c(t + t_0) \pm \pi/2]$, where t_0 corresponds to a known time of a maximum modulated signal. The receiver would multiply the incoming signal by $\cos \omega_c(t + t_0 \pm \Delta t)$ and average the result over one symbol period. The decision that the transmitted $\pi/2$ rad phase shift is plus or minus depends on whether the average is positive or negative. It is obvious from figure 1(b) that the average result is zero and no information is received
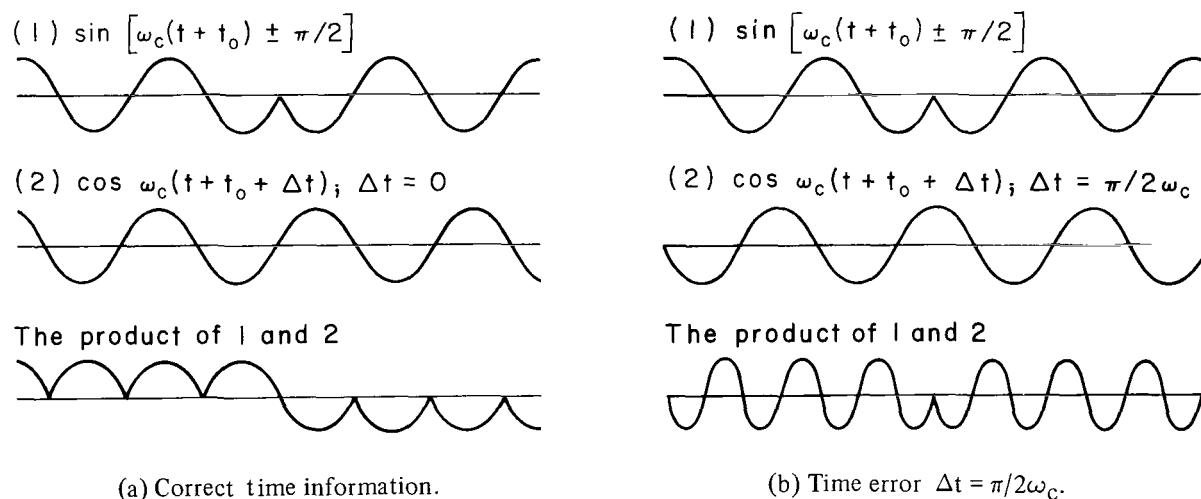

(1) $\sin\left[\omega_c(t + t_0) \pm \pi/2\right]$

(2) $\cos \omega_c(t + t_0 + \Delta t)$; $\Delta t = 0$

The product of 1 and 2

(a) Correct time information.

(1) $\sin\left[\omega_c(t + t_0) \pm \pi/2\right]$

(2) $\cos \omega_c(t + t_0 + \Delta t)$; $\Delta t = \pi/2\omega_c$

The product of 1 and 2

(b) Time error $\Delta t = \pi/2\omega_c$.

Figure 1.- Effect of incorrect time on phase detection.

if $\Delta t = \pi/2\omega_c$. It can be easily shown that if Δt is slightly greater than $\pi/2\omega_c$, the wrong decision would be made. Since $\Delta t = 10^{-6}$ implies that $\omega_c < \pi/2\times10^6$, then $\omega_c/2\pi = f_c$ would have to be less than 1/4 MHz for coherent detection, a frequency much too low for spacecraft communication. Therefore the relative time must be derived from the signal itself, which is the function of a phase tracking receiver. In the design of such a receiver oscillators are not as ideal as postulated for the above example. An oscillator has phase instability, and this instability can be modeled in terms of the above discussion by letting Δt be a random process instead of a fixed uncertainty. Thus, even with the phase tracking receiver, the question to be answered is: For a given signal frequency, what is the maximum variance of Δt that allows the detection process to be considered coherent? More specifically: How does performance differ from that of coherent detection as a function of Δt vs. $1/f_c$ or, equivalently, the ratio $\Delta t/T_c$ (where T_c is the period corresponding to f_c)? This ratio relates jitter in time to jitter in fractions of a cycle, but more conventionally, the ratio is multiplied by 2π to relate time jitter to radians of "phase" jitter. Note that frequency is a rate of change of phase; that is, $\omega_c \triangleq \Delta\phi/\Delta t$ or $\Delta\phi = \omega_c\Delta t = 2\pi\Delta t/T_c$; so the definitions are consistent. The rest of this discussion will concern time uncertainty expressed as phase jitter.

The first question regarding a telemetry system with coherent detection is: How much phase jitter can be tolerated before the system performance is degraded? Before one can answer that question the character of the phase jitter must be known.

Characterization of Phase Jitter

It should be emphasized at this point that discussing only "phase" jitter restricts the type of oscillators considered. In particular, the assumption is that the oscillator average frequency, denoted by

$$2\pi\bar{f} = \frac{1}{T} \int_0^T \left[\frac{d\phi(t)}{dt}\right] dt$$

does not drift in the interval of interest (up to 100 s). Thus the time waveform of the oscillator can be represented as

$$G \cos [2\pi\bar{f}t + \phi(t)], \qquad |\phi(t)| \leq \pi \text{ rad} \qquad (1)$$

where G is an arbitrary constant, t is time, and $\phi(t)$ is a realization of a random process (described as $\Delta\phi$ above) with an expected value $E(\phi) = 0$. The term $\phi(t)$ accounts for the difference between the actual time of zero crossing of the waveform and the expected time of zero crossing of the function $\cos 2\pi\bar{f}t$. If the waveform is phase modulated by a telemetry signal, it takes the form $M(t) = G \cos [2\pi\bar{f}t + \phi(t) + \theta(t)]$ where $\theta(t)$ is the telemetry information. A common way to characterize ϕ is by its power spectral

density, which is useful (for our purpose) because in the phase domain the telemetry information can be separated from the noise if the power spectral densities of each are compared. Let $S_\phi(\omega)$ be the power spectral density of $\phi(t)$. Many researchers in the field of oscillator stability have studied $S_\phi(\omega)$. The resulting characterization has been reported in references 1 and 2, which list numerous references, so the results will be stated here only briefly. The power spectral density of the phase jitter can be represented by the following polynomial:

$$S_\phi(\omega) = A/\omega^3 + B/\omega^2 \; C/\omega + D \tag{2}$$

in which A, B, C, and D are constants. The terms of the polynomial can be explained as follows.

Within the tuned circuit of an oscillator, perturbations (noise) cause frequency changes. Two sources of noise are characterized. Because of amplifier gain variations and variations in the crystal itself there is a flicker ($1/\omega$) component of noise and, because of thermally induced voltages in the circuit losses, there is a flat component of noise. Together these components form a *frequency* power spectral density $S_{\dot\phi}(\omega) = A/\omega + B$ $(rad^2/s^2)/rad$. Since $\omega = \dot\phi$, the equivalent *phase* power spectral density $S_\phi(\omega)$ can be derived from the *frequency* spectrum. The equivalence can be readily shown (although the method is not mathematically rigorous) using Fourier transform theory. The transform of $\dot\phi(t)$ is:

$$\Im[\dot\phi(t)] = j\omega\Im[\phi(t)] \tag{3}$$

but $2|\Im[\phi(t)]|^2$ can be termed the power spectral density, $S_\phi(\omega)$. Thus the power spectral density, $S_{\phi_i}(\omega)$, of the internally generated noise is

$$S_{\phi_i}(\omega) = \frac{1}{\omega^2} S_{\dot\phi}(\omega) = \frac{A}{\omega^3} + \frac{B}{\omega^2} \, rad^2/rad \tag{4}$$

Outside the tuned circuit, amplifiers and multipliers operate on the oscillator signal, and perturbations in these circuits cause phase jitter. These perturbations can also be either flat or $1/\omega$. This power spectral density is labeled $S_{\phi_o}(\omega) = C/\omega + D \, rad^2/rad$. If ϕ_i and ϕ_o are statistically independent, the combined power spectral density is

$$S_{\phi_i + \phi_o}(\omega) = A/\omega^3 + B/\omega^2 + C/\omega + D \, rad^2/rad$$

where the constants A, B, C, and D will be different for different circuits and also dependent on the choice of components.

Equation (2) gives an idea of the qualitative character of the modulation phase jitter. For large frequencies, $S_\phi(\omega)$ appears to be flat and for

components near D.C. it appears to be steeply rising. The assignment of quantitative values of phase jitter to the oscillators and carrier in the design of a telemetry system can only be done by measurement. Unfortunately the implementation of such a measurement is not easily accomplished.

The probability density function of phase jitter is gaussian with respect to some reference phase if the phase domain is unlimited. However, when dealing with periodic functions of phase, as in a phase tracking receiver, we think of phase as being restricted to the region from $-\pi$ to $+\pi$ radians; thus the density must be modified by "folding over the tails" of the gaussian probability density function. Viterbi's formulation (ref. 3, p. 90) for the modified probability density function is

$$p(\phi) = \frac{e^{\alpha \cos \phi}}{2\pi I_0(\alpha)}, \qquad |\phi| < \pi \qquad (5)$$

where I_0 is the zeroth-order modified Bessel function $I_0(\alpha) = \frac{1}{\pi} \int_0^\pi e^{\alpha \cos \theta} d\theta$ (see eq. 9.6.19, p. 376, ref. 4). In the ensuing discussion, a linear model will be assumed in which $\alpha = 1/\sigma_\phi^2$ and σ_ϕ^2 is the variance of ϕ. It should be realized that, for the operating range of interest for a phase tracking receiver ($\sigma_\phi < \pi/4$ is a reasonable bound for "in-lock" conditions), this density looks much like a gaussian density (see figs. 2 and 3).
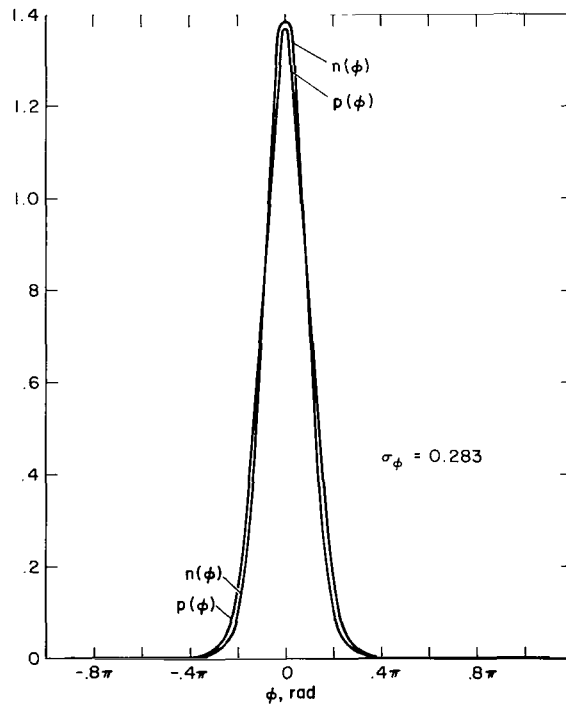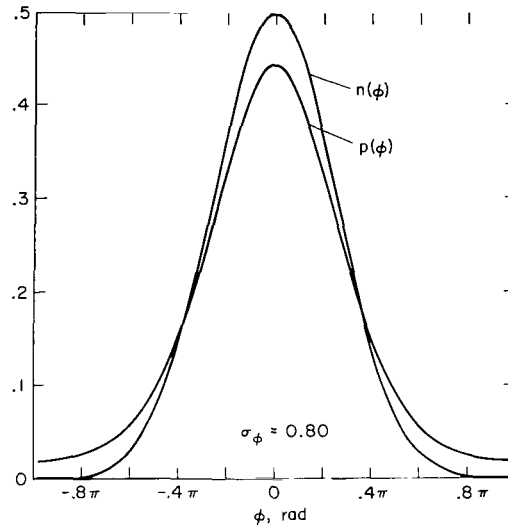

Figure 2.- Comparison plot of two formulations of the probability density function of phase jitter; $n(\phi) = \left(e^{-\alpha\phi^2/2}\right)/(2\pi/\alpha)^{1/2}$, $p(\phi) = (e^{\alpha \cos \phi})/2\pi I_0(\alpha)$, $\alpha = 1/\sigma_\phi^2$.

Figure 3.- Comparison plot of two formulations of the probability density function of phase jitter; $n(\phi) = \left(e^{-\alpha\phi^2/2}\right)/(2\pi/\alpha)^{1/2}$, $p(\phi) = (e^{\alpha\cos\phi})/2\pi I_0(\alpha)$, $\alpha = 1/\sigma_\phi^2$.

Total Phase Jitter in a Telemetry Receiver

The discussion so far has concerned the character of phase jitter in an oscillator or transmitter; now it will be shown how this jitter is manifested when filtered by a phase lock loop receiver. First, however, the functioning of a phase lock loop (PLL) will be reviewed. Although the receiver is more complex, it will be sufficient to assume it to be a simple second-order loop. The PLL tracks, or follows, both the phase and the frequency of a signal and effectively filters out all but a narrow band of noise centered on the signal frequency.

Three components are used to mechanize the PLL: A phase detector multiplies the input signal by a reference frequency to extract the relative phase error; a low pass filter removes all but the slowly varying or "D.C." components of the phase error; and a voltage controlled oscillator (VCO) generates the reference frequency for the phase detector. The VCO changes frequency in proportion to the output of the low-pass filter. A linear, phase domain model of the PLL will be used for analysis because it is directly applicable for small phase jitter, and the linear model is required for Fourier transform analysis. The phase-to-voltage transfer function of the phase detector is derived from the low-frequency part of the trigonometric identity

$$\sin(\omega_c t + \phi_i)\cos(\omega_c t + \phi_o) = 1/2\,\sin(\phi_i - \phi_o) + 1/2\,\sin(2\omega_c t + \phi_i + \phi_o)$$

6

and from the approximation $(\phi_i - \phi_o)$ small, $\sin(\phi_i - \phi_o) \simeq (\phi_i - \phi_o)$. The voltage-to-phase transfer function representing the VCO can be seen to include integration $1/j\omega$, since a voltage offset causes a frequency offset, which is a ramp in phase. Thus, we have the linear model:
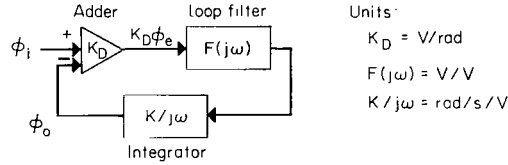
Sketch (a)

Define

$$H(j\omega) \equiv \frac{\phi_o(j\omega)}{\phi_i(j\omega)} = \frac{K_O K_D F(j\omega)}{j\omega + K_O K_D F(j\omega)} \tag{6}$$

and for simplicity let $K_D = 1$. Then

$$\frac{\phi_e}{\phi_i} \equiv \frac{\phi_i - \phi_o}{\phi_i} = 1 - H(j\omega) \tag{7}$$

For a second-order loop, $F(j\omega) = (j\omega\tau_2 + 1)/j\omega\tau_1$ (which provides proportional plus integral control), and the phase transfer function becomes

$$H(j\omega) = \frac{j\omega\tau_2 K/\tau_1 + K/\tau_1}{-\omega^2 + j\omega\tau_2 K/\tau_1 + K/\tau_1}$$

$$H(j\omega) = \frac{j\omega 2\delta\omega_n + \omega_n^2}{-\omega^2 + j\omega 2\delta\omega_n + \omega_n^2} \tag{8}$$

The phase error is

$$1 - H(j\omega) = \frac{\omega^2}{\omega^2 - j\omega 2\delta\omega_n - \omega_n^2} \tag{9}$$

where $\delta = (\tau_2/2)(K/\tau_1)^{1/2}$ is the loop damping factor ($\delta = 0.7$ for critical damping) and $\omega_n = (K/\tau_1)^{1/2}$ is the natural frequency of the loop. See figures 4 and 5.
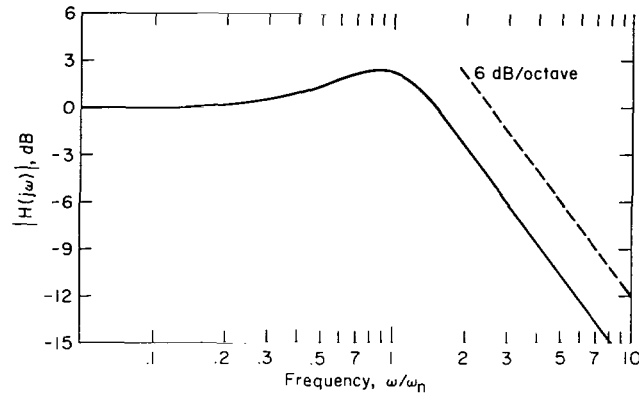
7

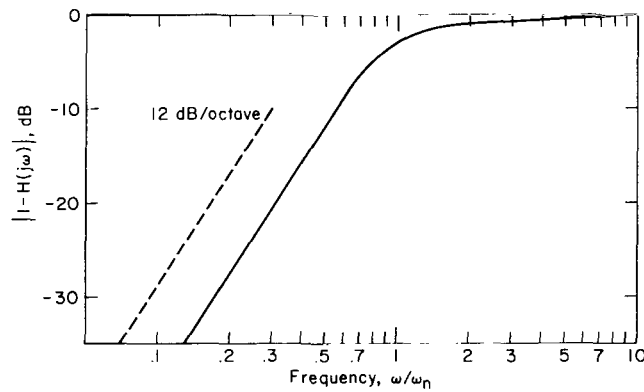Figure 4.- Phase transfer response for a high-gain, second-order loop where $\delta = 0.707$.

Figure 5.- Phase error response for a high-gain, second-order loop where $\delta = 0.707$.

To understand how these functions affect the total relative jitter in the receiver, one must differentiate between what we shall call internal and external sources of phase jitter on the incoming signal. "Internal" means phase jitter that is truly part of the signal as described in the previous section, and for simplicity it includes any inherent VCO instability since we are concerned with relative jitter between signal and VCO. "External" jitter means phase jitter arising from thermal noise and is inversely proportional to the signal-to-noise ratio in the receiver PLL. The portion of these types of jitter which appear at the receiver phase detector will be designated ϕ_{in} and ϕ_x, respectively.

The frequency spectrum S_{ϕ_x} is flat and the portion near the signal frequency is tracked out by the receiver. Thus the total power out of the receiver phase detector due to this phase jitter is proportional to

8

$$\overline{\phi_x^2} = \int_0^{\omega_{if}} S_{\phi_x}(\omega) \left| H(j\omega) \right|^2 d\omega$$

$$= S_{\phi_x} \int_0^{\omega_{if}} \left| H(j\omega) \right|^2 d\omega \tag{10}$$

or

$$\overline{\phi_x^2} = (2\pi B_L) S_{\phi_x} \equiv \frac{1}{2} \left(\frac{N}{S} \right)_L \tag{11}$$

where $(N/S)_L$ is defined as the noise-to-signal ratio measured in the loop (ref. 5), B_L is the standard definition of a single sided noise power bandwidth for a PLL, and ω_{if} is half the intermediate frequency bandwidth in rad/s. For $\omega_{if} \geq 100 \omega_n$, and with a critically damped PLL, $B_L = 0.53\omega_n$ Hz (ref. 5). (The bandwidth limitation ω_{if} is due to the intermediate frequency bandpass of the receiver which may be thought of as prefiltering the linear model of the PLL.)

The frequency spectrum $S_\phi(\omega)$ as described in the previous section is

$$S_\phi(\omega) = \frac{A}{\omega^3} + \frac{B}{\omega^2} + D$$

(the C term is negligible in most oscillators) and the portion of this spectrum which appears as phase jitter in the receiver is that which is *not* tracked by the PLL (i.e., the phase error). Thus the total power out of the receiver phase detector due to this phase jitter is proportional to

$$\overline{\phi_{in}^2} = \int_0^{\omega_{if}} S_\phi(\omega) \left| 1 - H(j\omega) \right|^2 d\omega \tag{12}$$

The exact computation of this integral is tedious, but the result can be bounded and the important terms can be found by approximating the phase error function from figure 4. Let $\left| 1 - H(j\omega) \right| \simeq (\omega^2/\omega_n^2)$ for $\omega \leq \omega_n$, and let $\left| 1 - H(j\omega) \right| \simeq 1$ for $\omega > \omega_n$. The approximation to the above integral is defined by $\overline{U_{in}^2}$:

$$\overline{U_{in}^2} = \int_0^{\omega_n} S_\phi(\omega) |1 - H(j\omega)|^2 \, d\omega + \int_{\omega_n}^{\omega_{if}} S_\phi(\omega) |1 - H(j\omega)|^2 \, d\omega$$

$$= \int_0^{\omega_n} \left(\frac{A}{\omega^3} + \frac{B}{\omega^2} + D\right)\left(\frac{\omega^2}{\omega_n^2}\right)^2 d\omega + \int_{\omega_n}^{100\omega_n} \left(\frac{A}{\omega^3} + \frac{B}{\omega^2} + D\right)(1)^2 d\omega$$

$$= \frac{1}{\omega_n^4} \int_0^{\omega_n} (A\omega + B\omega^2 + D\omega^4) \, d\omega + \int_{\omega_n}^{100\omega_n} \left(\frac{A}{\omega^3} + \frac{B}{\omega^2} + D\right) d\omega$$

$$= \frac{1}{\omega_n^4}\left[\frac{A\omega^2}{2} + \frac{B\omega^3}{3} + \frac{D\omega^5}{5}\right]_0^{\omega_n} + \left[\frac{-A}{2\omega^2} - \frac{B}{\omega} + D\omega\right]_{\omega_n}^{100\omega_n}$$

$$= \left[\frac{A}{2\omega_n^2} + \frac{B}{3\omega_n} + \frac{D\omega_n}{5}\right] + \left[\frac{A}{2\omega_n^2} - \frac{A}{2\times10^4\omega_n^2} + \frac{B}{\omega_n} - \frac{B}{100\omega_n} - D\omega_n + 100D\omega_n\right]$$

$$\tag{13}$$

Neglecting terms in A, B, and D of 1% or less,

$$\overline{U_{in}^2} = \frac{A}{2\omega_n^2} + \frac{A}{2\omega_n^2} + \frac{B}{3\omega_n} + \frac{B}{\omega_n} + 100D\omega_n \tag{14}$$

or

$$\overline{U_{in}^2} = \frac{A}{\omega_n^2} + \frac{4B}{3\omega_n} + 100D\omega_n \quad \text{radians}^2$$

Then

$$U_{RMS} = \sqrt{\frac{A}{\omega_n^2} + \frac{4B}{3\omega_n} + 100D\omega_n} \quad \text{radians} \tag{15}$$

where

$$U_{RMS} \equiv \sqrt{\overline{U_{in}^2}}$$

From measurements on the Pioneer spacecraft transmitter (see measurement results, p. 22) typical numbers can be assigned to the constants A, B, and D at S-band frequency to give a better perspective of the important terms for a narrow PLL ($2B_L < 100$ Hz). Typical values are $A = 0.5$ rad^5/rad, $B = 10^{-3}$ rad^4/rad, $D = 2\times10^{-10}$ rad^2/rad. Thus the A term clearly dominates for $\omega_n < 100$ rad. Figure 6 shows that the approximation for $|1 - H(j\omega)|(A/\omega^3)$ is an upper bound for this term. It has been shown by approximation that only
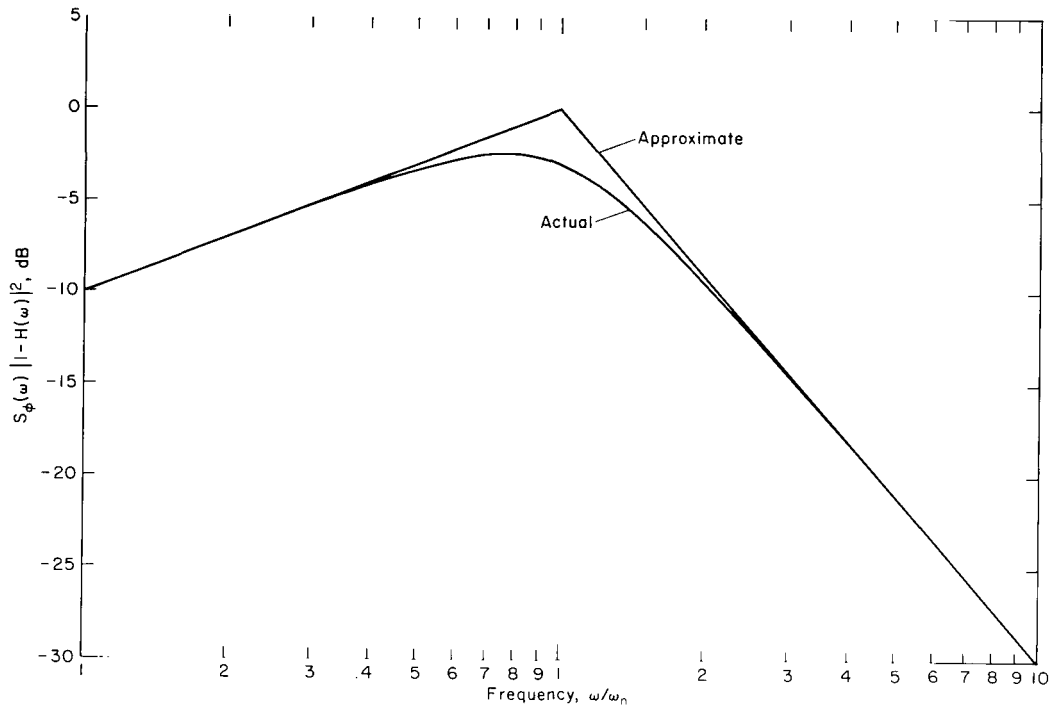
Figure 6.- Power spectral density (PSD) for the relative phase error in a phase lock loop where the predominate phase jitter has PSD form A/ω^3. The PSD is in dB relative to A/ω_n^3.
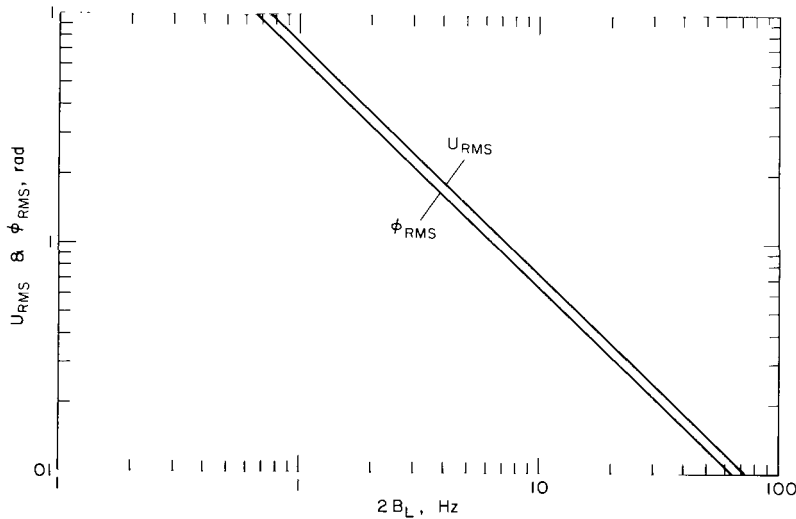

Figure 7.- Total RMS phase jitter in a phase lock loop where the PSD of the relative phase jitter is $0.5/\omega^3$ rad^2/rad.

the A term is important, and fortunately its contribution to ϕ_{RMS} can be calculated accurately (see appendix A). Figure 7 shows U_{RMS} and ϕ_{RMS} for the A term versus $2B_L$.

The value of separating the two components of phase jitter lies in exposing conditions under which oscillator instability or $\overline{\phi_{in}^2}$ must be considered in the design of the threshold loop bandwidth of a receiver. Normally the receiver design threshold

11

is based on only the signal-to-noise ratio in the loop or $\overline{\phi_x^2}$. In most receivers the phase detector is preceded by a bandpass limiter which suppresses the signal and thereby reduces the loop bandwidth at signal-to-noise ratios near threshold. Therefore it is not surprising that ϕ_{in} can be a small phase jitter under strong signal conditions (where $2B_L$ is large) and still be large enough to reduce performance from the design value when the receiver is near threshold (where $2B_L$ is small). Note the 10-times increase in ϕ_{RMS} for a 10 to 1 change in $2B_L$ in figure 7.

Effect of Internal Phase Jitter on PCM Telemetry Performance

In order to calculate the effect of internal phase jitter on telemetry performance, several assumptions are needed to further define the problem and limit the complexity of the solution:

1. The receiver acts as a single conversion type with the PLL phase detector operating at the carrier frequency. The PLL is a second-order type critically damped as described in the previous section.

2. The effect of receiver thermal noise in the tracking loop bandwidth will be ignored for this part of the discussion (i.e., only ϕ_{in} is considered).

3. No differentiation will be made between phase jitter originating in the transmitter and that originating in the receiver. All the jitter is shown in the receiver VCO. For the purpose of calculating the effect on telemetry error rate, only the relative jitter is of concern.

4. The problem of subcarrier demodulation will be considered negligible; therefore the carrier input to the telemetry phase detector is modeled as being directly phase modulated with PCM. Also, perfect bit synchronization is assumed. The block diagram of the model is:
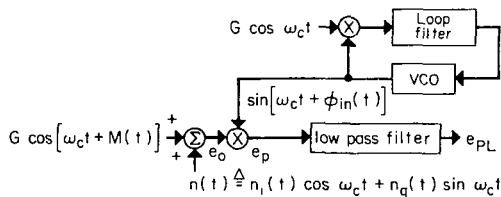
Sketch (b)

In the model, n(t) is the receiver additive noise represented by its in-phase and quadrature components, and e_{PL} is the baseband telemetry signal. Thus

$$e_o = G \cos [\omega_c t + M(t)] + n_i(t) \cos \omega_c t + n_q(t) \sin \omega_c t \qquad (16)$$

$$e_p = e_o \sin [\omega_c t + \phi(t)] \qquad (17)$$

(For simplicity the subscript "in" is dropped from $\phi(t)$.) Using trigonometric identities and neglecting higher frequency terms (the low pass filter removes all high order terms):

12

$$e_{PL} = \frac{G}{2} \sin [\phi(t) + M(t)] + \frac{n_i(t)}{2} \sin \phi(t) + \frac{n_q(t)}{2} \cos \phi(t) \qquad (18)$$

but the first term can be written

$$\frac{G}{2} \cos \phi(t) \sin M(t) + \frac{G}{2} \sin \phi(t) \cos M(t)$$

Note:

$$M(t) = \pm d \text{ for PSK; } \cos \pm d = \cos d \overset{\Delta}{=} \gamma \qquad (\gamma \text{ is a constant})$$

Then

$$e_{PL} = \frac{G}{2} \sin M(t) \cos \phi(t) + \frac{G}{2} \gamma \sin \phi(t) + \frac{n_i(t)}{2} \sin \phi(t) + \frac{n_q(t)}{2} \cos \phi(t)$$

In the above equation

1. $\frac{G}{2} \gamma \sin \phi(t)$ has a noise spectrum near DC, but in practice the data are on a subcarrier; thus this term is filtered out.[1]

2. $\frac{n_i(t)}{2} \sin \phi(t) + \frac{n_q(t)}{2} \cos \phi(t)$ is an expansion of $\frac{n(t)}{2}$ as shown in sketch (b).

Therefore

$$e_{PL} = \frac{G}{2} \sin M(t) \cos \phi(t) + \frac{n(t)}{2} \qquad (19)$$

where $G \sin M(t) = \pm K$; the magnitude of K is determined by the modulation index and the sign determined by the telemetry (+ corresponds to one; - corresponds to zero).

For correlation and matched filter detection of a binary signal such as this, the following decision variable is formed:

$$q_k = \int_O^T [(\pm K \cos \phi(t) + n(t))] dt$$

$$= \pm K \int_O^T \cos \phi(t) dt + \int_O^T n(t) dt \qquad (20)$$

The symbol "one" is sent if q_k is positive or "zero" if q_k is negative.

Now

$$P_e = Pr(error) \text{ where } Pr(\cdot) \text{ is the probability of the event } (\cdot).$$

[1]This is strictly true only for small $\phi(t)$ where $\sin \phi(t) \simeq \phi(t)$. With $\sigma_\phi = \pi/4$, the $\sin \phi(t)$ will have energy at harmonics of the bandwidth of $\phi(t)$, but only the higher harmonics would be in the bandpass of the subcarrier, and they are small enough to be neglected.

Then

$$P_e = Pr(1) \ Pr(error/1) + Pr(0) \ Pr(error/0)$$

Also, by symmetry,

$$Pr(error/1) = Pr(error/0) \ and \ Pr(1) + Pr(0) = 1$$

thus

$$P_e = Pr(error/1)$$

Therefore it is necessary to use only

$$q_1 = K \int_0^T \cos \phi(t) \ dt + \int_0^T n(t) dt \qquad (21)$$

To calculate the error probability, q_1 can be normalized by multiplying by $1/KT$ without changing the decision point; then

$$q = \frac{1}{T} \int_0^T \cos \phi(t) dt + \frac{1}{TK} \int_0^T n(t) dt \qquad (22)$$

and

$$P_e = Pr(error/1) = \int_{-\infty}^0 p_q(x) dx$$

where $p_q(x)$ is the probability density function of q. Unfortunately, finding the probability density of q is not easy. As can be seen from the above equation, q is the sum of two random variables which we will assume to be independent.

The second term, $\frac{1}{TK} \int_0^T n(t) dt$, is the random variable derived from a white gaussian process; it also is gaussian with zero mean and variance $\sigma^2 = N_0/2K^2T$. (N_0 = single-sided density; see appendix D for evaluation of this term.)

The probability density function of the sum can be found by convolution (see appendix E):

$$p_q(x) = \int_{-\infty}^\infty h(x-u) g(u) du \qquad (23)$$

If $\phi(t)$ is small (i.e., $\phi(t) \ll 1$) $g(x)$ approaches a delta function at $x = 1$, then $p_q(x)$ is a gaussian density with mean one. We know that for a gaussian $p_q(x)$, P_e is the error function for coherent PSK given by

14

$$P_e = \int_{-\infty}^{0} \frac{1}{\sigma\sqrt{2\pi}} \, e^{\frac{-(x-1)^2}{2\sigma^2}} \, dx, \qquad \sigma^2 = \frac{N_o}{2K^2T}$$

By a change of variable, this can be written

$$P_e = \frac{1}{\sqrt{\pi}} \int_{-\infty}^{-\frac{1}{\sqrt{2}\sigma}} e^{-v^2} dv \qquad \text{(ref. 6)} \tag{24}$$

Finding the probability density function of the first term is the main problem. The probability density function of $\frac{1}{T} \int_{o}^{T} \cos \phi(t)dt$ has not been found in general for the case where $S_\phi(\omega)$ is arbitrary and $\phi(t)$ is assumed to be a gaussian process (see appendix B). Therefore, the analysis will be restricted to the case when the symbol period T is short compared to the time required for $\phi(t)$ to change appreciably.

Symbol rates larger than the loop noise bandwidth are the main concern because the performance degradation for coded telemetry is of primary interest and the symbol rate for coding is relatively high. To illustrate this point, let $P_e = 0.001$, corresponding to a normalized signal-to-noise ratio of 6.8 dB. If the loop bandwidth were equal to the symbol bandwidth and the power split equally between the carrier and the symbol, the loop signal-to-noise ratio would be at threshold (6 dB) which means, of course, that the receiver would hardly maintain lock. Actually lower symbol signal-to-noise ratios are used and less power is allowed for the carrier. Thus to maintain a higher signal-to-noise ratio in the loop, the loop bandwidth would always be a fraction of the symbol rate.

Under these conditions $\cos \phi(t)$ is practically constant over the integration interval T. Thus the following approximation holds (see appendix B):

$$\frac{1}{T} \int_{o}^{T} \cos \phi(t)dt \simeq \frac{1}{T} \cos \phi(t) \int_{o}^{T} dt = \cos \phi(t) \tag{25}$$

and its probability density function is easily calculated (see appendix C):

$$g(\cos \phi) \stackrel{\Delta}{=} g(z) = \frac{e^{\alpha z}}{\pi I_o(\alpha) \sqrt{1-z^2}} , \qquad |z| < 1 \tag{26}$$

where

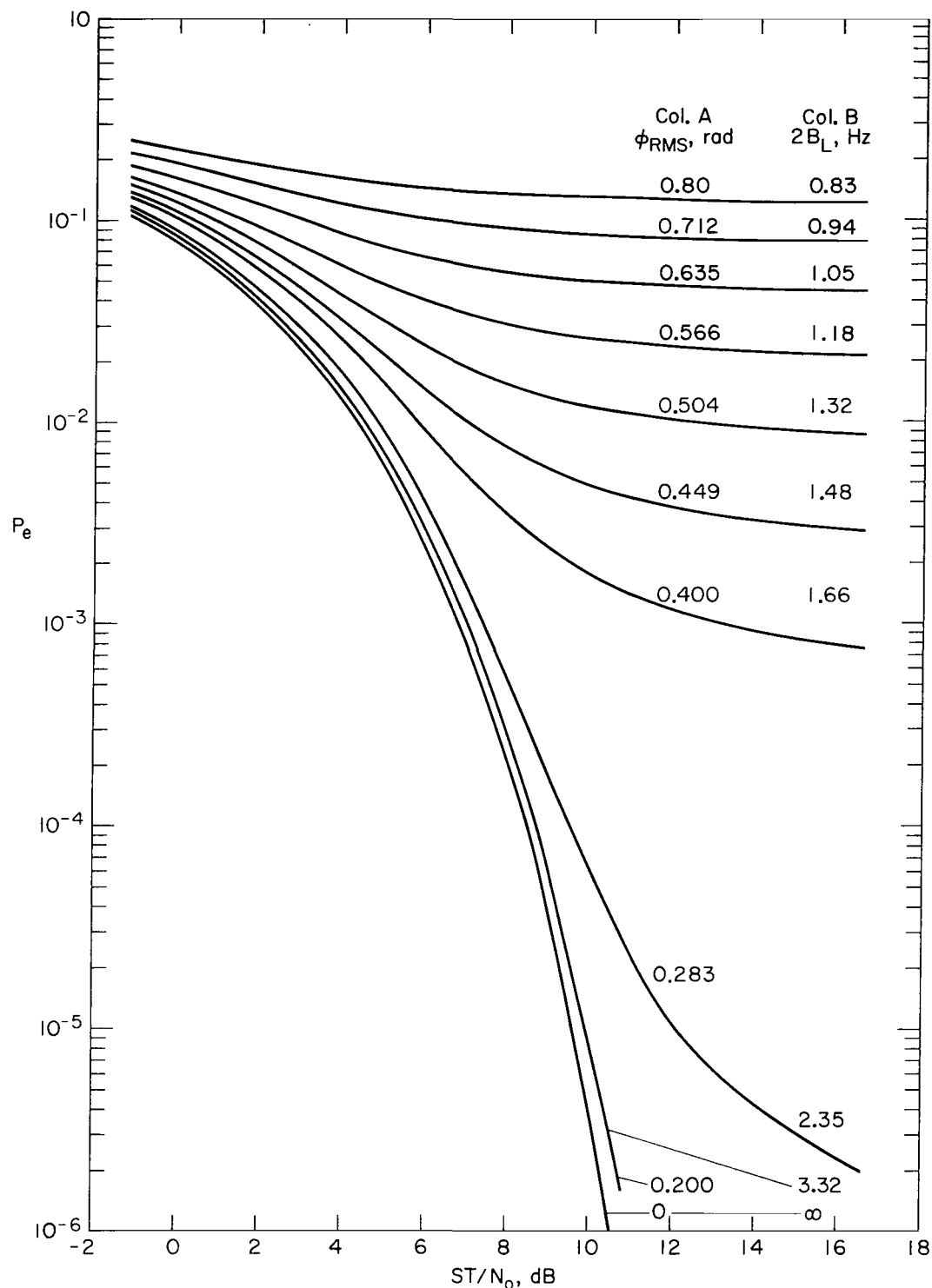$$\alpha = \frac{1}{\sigma_\phi^2} = \frac{1}{\phi_{in}^2}$$

15

Figure 8.- Parametric error rate curves showing the effect of phase jitter. Column A labels the curves for different values of total RMS relative phase jitter between the carrier signal and the receiver VCO. Column B labels the curves for different receiver loop bandwidths ($2B_L$) assuming that the dominant source of relative phase jitter is that which was measured on Pioneer VI — IX type of transmitter.

From physical reasoning $g(z)$ is expected to be a function of the general shape shown in sketch (c). The mean value of $\phi(t)$ is zero, and the highest probability of $\phi(t)$ occurs in the region about zero. Since $\cos \phi(t)$ is approximately 1 in this region, the highest probability of $\cos \phi(t)$ occurs near 1. The probability of realizing larger values of the magnitude of $\phi(t)$ decreases smoothly according to the gaussian process, as the magnitude of $\phi(t)$ increases. Therefore, the probability density of $\cos \phi(t)$ would be expected to decrease smoothly as $|\phi(t)|$ increases.
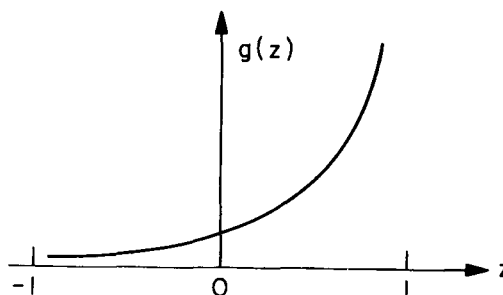
Sketch(c)

This form for the phase jitter has been used to evaluate

$$P_e = \int_{-\infty}^{0} h(x) * g(x) \, dx$$

on a computer for various values of

$$\sigma = \sqrt{\frac{N_O}{2K^2T}} \quad \text{and} \quad \sigma_\phi = \sqrt{\overline{\phi_{in}^2}} \triangleq \phi_{RMS}$$

(See appendix E for the details.) Figure 8 illustrates the results.

Three important conclusions can be derived from the results. First, if the total phase jitter is low ($\phi_{RMS} < 0.28$ rad), the telemetry performance is nearly ideal over the range of P_e of interest ($P_e > 5\times10^{-4}$). The performance

matches the theoretical error curve for coherent PSK within 0.2 dB for ϕ_{RMS} = 0.2 rad. Second, for higher values of total phase error, the normalized signal-to-noise ratio for the telemetry symbols rapidly loses influence on the error rates. It can be shown that for a given ϕ_{RMS} there is a P_e which cannot be reduced by any increase in signal strength (see appendix E). For example, if ϕ_{RMS} = 0.56, the minimum P_e attainable would be approximately 2.0×10^{-2}. Third, in figure 6, which is drawn for oscillators such as those in Pioneer VI through IX, it should be observed that ϕ_{RMS} is inversely proportional to the receiver loop bandwidth in the range of interest ($2B_L \leq 12$ Hz). Thus, for any given maximum allowable probability of error in telemetry, a minimum receiver loop bandwidth is established. For other oscillators and other ranges of P_e and $2B_L$, a proportional relationship between $2B_L$ and ϕ_{RMS} will not be given in general; however, the same min-max relationship exists between $2B_L$ and P_e. Fortunately, this bound often lies outside the range of P_e and $2B_L$ of interest to the designer. For Pioneer telemetry, the receivers currently used have a minimum loop bandwidth of 3 Hz and thus the effect of Pioneer oscillator instability on the telemetry is negligible as shown by the analysis results in figure 8 column B.

THE OSCILLATOR INSTABILITY MEASUREMENT SYSTEM

The difficulty in measuring $\phi(t)$ is that one must generate a reference carrier equivalent to that of the test oscillator but without the $\phi(t)$ phase jitter. As has been demonstrated above, in communications a time reference must be generated to measure or extract any phase modulation, including PM telemetry. In fact, the precision reference source built to extract $\phi(t)$ contains a phase lock loop, just as a coherent PM receiver is basically a PLL. Of course, the design is different because the emphasis is on reducing the self-induced phase jitter to a minimum and on having a high sensitivity to phase variations. The resultant extracted phase jitter is the sum of the jitter from the two sources, and hopefully the phase jitter from the measuring instrument will be small. One such device was developed and built, under NASA-Ames contract, to measure phase noise in the telemetry link for the Pioneer series of spacecraft. It is called an Oscillator Instability Measurement System (OIMS), and consists of an extraction section

18

Figure 9.- OIMS extraction section.

(see fig. 9) that extracts phase jitter from an intermediate carrier frequency
of 10 MHz ±1 percent and a frequency conversion section that mixes various
carriers, used in the Pioneer telemetry link, down to 10 MHz. To understand
the design, one salient point must be demonstrated about phase jitter. If
the passband for the carrier is always broad with respect to $S_\phi(\omega)$ and the
carrier frequency is multiplied by n, via a nonlinear device

$$A \cos n[2\pi \overline{f} t + \phi(t)] = A \cos[2\pi n \overline{f} t + n\phi(t)] \tag{27}$$

which means that the power spectral density $S_\phi(\omega)$ is scaled up by n^2, but the
envelope shape is unchanged. Likewise, if n is less than 1, say $n \triangleq 1/D$,
$S_\phi(\omega)$ is scaled down by $1/D^2$. For low phase jitter, the PLL for the OIMS has
been built around a frequency standard with low phase jitter. Mixing its
frequency with a relatively noisy synthesized frequency, which is partly
voltage controlled and frequency divided by $D = 100$ $(1/D^2 = 10^{-4})$, produces
a combined frequency which is variable. The divided synthesized component
has a low phase jitter, and therefore the phase jitter is still small compared
to most oscillators.

Figure 9 shows in detail how the extraction section of the OIMS functions. The 10 ±0.1 MHz reference is composed of two sources; a 9 MHz signal which has the stability of the frequency standard, and a 1 ±0.1 MHz signal which has components from the standard, the synthesizer, and a voltage controlled oscillator or VCO (which is physically part of the synthesizer). In this simple block diagram a linear model is used to describe the nonlinear elements that add and subtract, and scale frequencies up or down. Filtering and buffering requirements are not shown in the diagram.

The 9 MHz signal is generated by simultaneously scaling the 5 MHz from the standard up to 10 MHz and down to 1 MHz, then taking the difference. The other component of the reference 1.0 ±0.1 MHz signal is generated by combining the 5 MHz standard, scaled up to 60 MHz, with the 40 ±10 MHz output of the frequency synthesizer. This produces a 100 MHz ±10 MHz signal which is scaled down to 1 ±0.1 MHz. The frequency of the synthesizer output can be selected manually over a range of ±10 MHz and has automatic tracking, via the PLL, of up to 10 KHz from the VCO in the kilohertz decade of the synthesizer. This range, of course, is scaled down to ±0.1 MHz and 100 Hz, respectively.

The extraction section has three outputs which are limited to baseband frequencies. Each is buffered by low-pass filtering amplifiers (not shown) with variable gain , but only the most sensitive output transfer functions are indicated. The only output of concern to this discussion is labeled PM for the extracted "phase modulating" signal or equivalently phase jitter. The extractor also outputs the related "frequency modulating" or FM signal and a signal proportional to any incidental "amplitude modulation" (AM).

The 10 MHz reference, which is generated as described above, will track the phase and frequency of the signal under test without introducing much phase jitter of its own. Figure 10 shows the residual power spectral density of phase jitter for the OIMS extraction section when operated in a self-test or common mode condition.[2] Under this condition the frequency standard also provides the signal to be tested and thus only the phase jitter due to the PLL amplifiers, phase detector, VCO, and synthesizer is displayed.

Figure 11 shows the power spectral density of the phase jitter for a similar external frequency standard as extracted by the OIMS at 10 MHz. If one can neglect the residual, and both standards contribute equally to the

---

[2]Note that these plots, which were taken directly from low frequency spectrum analyzers, are in units of $S_\phi(f)$ rad^2/Hz versus Hertz. The conversion to $S_\phi(\omega)$ is simple if one remembers that the power in a fixed bandwidth is the same, then

$$\Delta f_c S_\phi(f) = \Delta \omega_c S_\phi(\omega)$$
$$\Delta f_c S_\phi(f) = \Delta(2\pi f_c) S_\phi(\omega)$$

therefore

$$S_\phi(f) = 2\pi S_\phi(\omega) \tag{28}$$

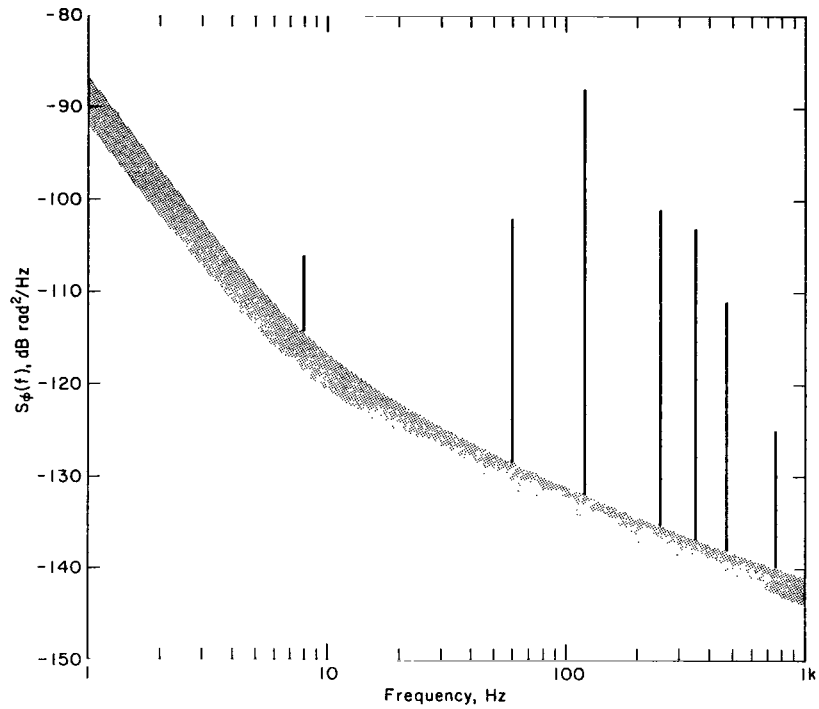The crosshatched area indicates the band of uncertainty in the measurement.

Figure 10.- OIMS common mode power spectral density, $S_\phi(f)$, of residual phase jitter. Spectral lines shown are harmonics of the AC power frequency.
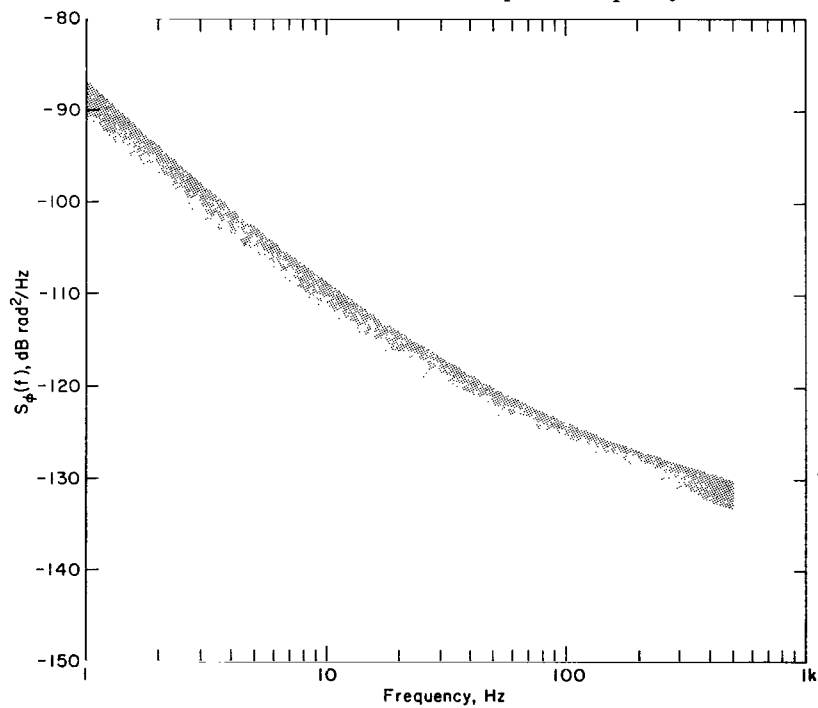

Figure 11.- OIMS extraction of $S_\phi(f)$ for a frequency standard referred to 10 MHz. Spectral lines are omitted for clarity.

21

jitter, the amount associated with the OIMS standard is 3 dB less than this plot. Note that the phase jitter of the standard is greater than the common mode residual.

The other section of the OIMS is the frequency conversion section (not shown) and its function is to heterodyne, up or down, signals under test into the range of the extractor (10 ±0.1 MHz). The phase jitter on the local oscillator in the converter also must be as low as possible since, when it is mixed with the signal under test, the resulting phase jitter power is the sum of that originating in the local oscillator and from the input signal. Thus all the local oscillator frequencies needed for tests are directly synthesized in the converter from the frequency standard used in the extractor section. Synthesis is performed in the same way as for the frequencies needed in the extractor, so the frequency converter is not described in detail.

MEASUREMENT OF PIONEER OSCILLATION STABILITY

Most measurements of the Pioneer oscillator stability were made at the intermediate frequency of 114.6 MHz. Thus a mixing or local oscillator (LO) frequency of 104.6 MHz was generated for this purpose in the frequency converter. The frequency multiplying and mixing from the standard's frequencies (5 MHz, 1 MHz, and 100 KHz) are represented by the following equation: LO = [(20×5) + (4×1) + (6×0.1)] MHz. The phase jitter on this local oscillator is dominated by the first term of 100 MHz. As was explained above, the phase jitter of this term has the same spectral shape as that of the frequency standard (fig. 11), but the magnitude is scaled up by $n^2 = 10^2$ or 20 dB.

Figure 12 shows a plot of $S_\phi(f)$ vs f for the Pioneer oscillator taken directly from OIMS measurements of several oscillators of the same design; notice that the spectrum is considerably above S_ϕ for the local oscillator for frequencies below 100 Hz; thus the correct measurement of the Pioneer oscillator phase jitter is assured in this region. Also notice that the shape of S_ϕ for frequencies below 100 Hz is $1/f^3$. The rapid roll-off of S_ϕ for frequencies above 1.5 KHz is caused by narrow band-pass filtering of the output of the Pioneer oscillator. It is this plot that provides the basis for the terms A, B, and D used in the calculation of the total phase jitter in the Analysis section.

From measurements made with the OIMS it was possible to simplify the general problem of calculating the effects of phase jitter on the telemetry performance by neglecting terms in the polynomial for the power spectral density. Knowing the actual magnitude and power spectral density of the telemetry oscillator phase jitter made it possible not only to solve the specific problem of determining the oscillator's effect on Pioneer telemetry, but to draw general conclusions about conditions under which oscillator phase jitter is a critical parameter.
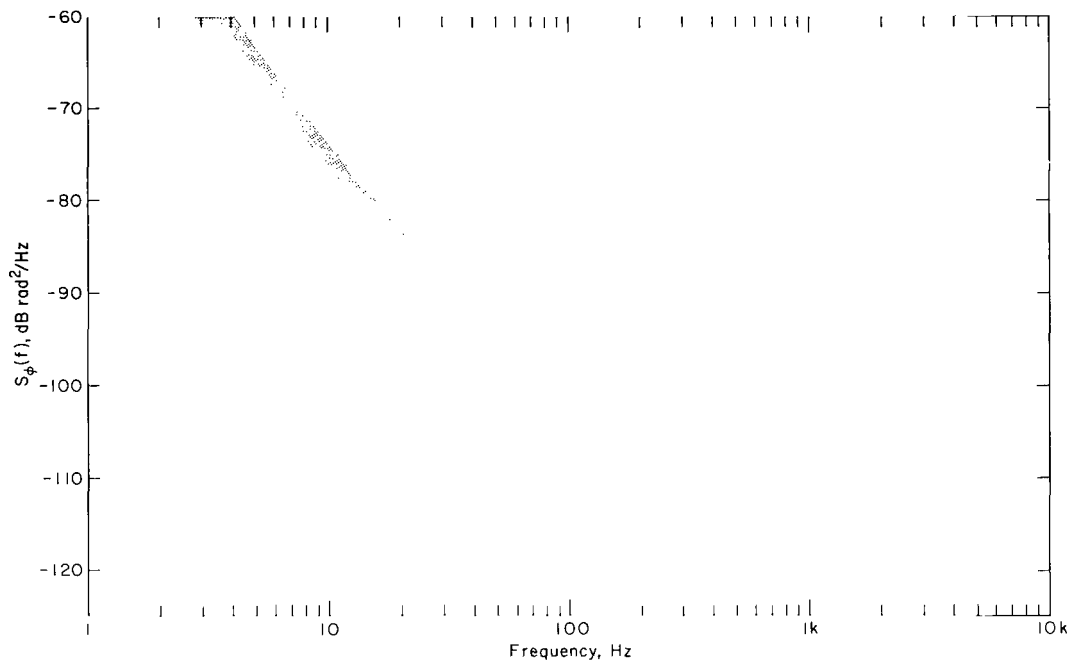
22

Figure 12.- OIMS conversion and extraction of $S_\phi(f)$ for a Pioneer VI-IX type of transmitter oscillator multiplied in frequency to 114.6 MHz. Spectral lines are omitted for clarity.

CONCLUDING REMARKS

It has been shown quantitatively that short-term oscillator instability degrades telemetry performance. Instability was defined as a phase jitter with a general power spectral density, $S_\phi(\omega) = A/\omega^3 + B/\omega^2 + C/\omega + D$, and the oscillator instability measurement system for extracting the phase jitter of an oscillator was described. The instability in the Pioneer VI through IX telemetry transmitter circuits was used as an example, to derive an expression for the total phase jitter expected from a telemetry receiver as a function of receiver loop bandwidth. Finally it was predicted analytically that even under strong signal conditions, oscillator instability can degrade telemetry performance if the receiver loop bandwidth is narrow. Unfortunately the complete theory was not verified with data since in the Pioneer telemetry system the effect of phase jitter was negligible.

The oscillator instability measurement system was key to these results. Measurement of the power spectral density of the phase jitter on the oscillator was a necessary first step. The problem of the effect of oscillator instability on telemetry is too broad a topic to treat generally, and data were needed to limit the parameters properly. The problem has been solved for a specific

23

case in great detail so that it will be easy to apply the results with confidence to another similar telemetry problem.

Ames Research Center
    National Aeronautics and Space Administration
        Moffett Field, Calif., 94035, March 11, 1971

APPENDIX A

CALCULATION OF THE MEAN SQUARE VALUE OF THE
INTERNAL PHASE JITTER

In the Analysis section, the expression for the phase jitter in a phase lock receiver was derived. Presented here is the evaluation of the integral for the phase jitter, which is given by:

$$\overline{\phi_{in}^2} = \int_0^{\omega_{if}} S_\phi(\omega) |1 - H(j\omega)|^2 d\omega \tag{A1}$$

The above expression represents the total phase jitter of ϕ_{in} in the sum-of-squares sense. It also represents the variance of ϕ_{in} if ϕ_{in} is a process with zero mean; a third interpretation of ϕ_{in}^2 would be that it is the modulation power loss on a carrier frequency due to oscillator phase jitter. The term $S_\phi(\omega)$ is the single sided "power" spectral density of ϕ_{in} and has units of radians² per radian. To relate $S_\phi(\omega)$ to a measurement made using the OIMS (see p. 18), it should be noted that $S_\phi(\omega) = (1/2\pi) S_\phi(f)$ where $S_\phi(f)$ has units of radians² per Hertz. Since $S_\phi(f)$ is measured by a sweeping wave analyzer, which sweeps only positive frequencies, $S_\phi(f)$ is twice the density used when integrations are made over the whole frequency domain.

To evaluate the integral, expand $1 - H(j\omega)$ and write the square of its magnitude

$$|1 - H(j\omega)|^2 = \left| \frac{\omega^2}{\omega^2 - j\omega^2 \delta\omega_n - \omega_n^2} \right|^2 \tag{A2}$$

Since

$$\left| \frac{z_1}{z_2} \right| = \frac{|z_1|}{|z_2|} \ , \quad |1 - H(j\omega)|^2 = \frac{|\omega^2|^2}{|\omega^2 - j\omega^2 \delta\omega_n - \omega_n^2|^2}$$

and $|z|^2 = zz*$ where $z*$ is the complex conjugate of z. Thus

$$|1 - H(j\omega)|^2 = \frac{\omega^4}{(\omega^2 - \omega_n^2)^2 + 4\delta^2\omega_n^2\omega^2}$$

$$= \frac{\omega^4}{(\omega^4 - 2\omega_n^2\omega^2 + \omega_n^4) + 4\delta^2\omega_n^2\omega^2}$$

But for a critically damped PLL, $2\delta = \sqrt{2}$, $4\delta^2 = 2$; thus

$$\left|1 - H(j\omega)\right|^2 = \frac{\omega^4}{\omega^4 + \omega_n^4} \tag{A3}$$

The other factor in the integrand is $S_\phi(\omega)$ which has been shown to have the general expression $A/\omega^3 + B/\omega^2 + C/\omega + D$. However, approximations show that for loop bandwidths of interest, only the A-term in $S_\phi(\omega)$ is significant; thus

$$\overline{\phi_{in}^2} = \int_0^{\omega_{if}} \frac{A}{\omega^3}\left(\frac{\omega^4}{\omega^4 + \omega_n^4}\right)d\omega$$

$$= \int_0^{\omega_{if}} \left(\frac{A\omega}{\omega^4 + \omega_n^4}\right)d\omega \tag{A4}$$

Performing a change of variable, let $z = \omega^2$; then $dz = 2\omega\,d\omega$ and for $0 \le \omega \le \omega_{if}$, $0 \le \sqrt{z} \le \omega_{if}$, or $0 \le z \le \omega_{if}^2$

$$\overline{\phi_{in}^2} = \frac{A}{2}\int_0^{\omega_{if}} \frac{2\omega\,d\omega}{\omega^4 + \omega_n^4}$$

$$= \frac{A}{2}\int_0^{\omega_{if}^2} \frac{dz}{z^2 + \omega_n^4}$$

$$= \frac{A}{2}\left[\frac{1}{\omega_n^2}\tan^{-1}\frac{z}{\omega_n^2}\right]_0^{\omega_{if}^2} \qquad \text{(ref. 7, p. 294)} \tag{A5}$$

$$\overline{\phi_{in}^2} = \frac{A}{2\omega_n^2}\tan^{-1}\frac{\omega_{if}^2}{\omega_n^2} \tag{A6}$$

so that

$$\phi_{RMS} \triangleq \sqrt{\overline{\phi_{in}^2}} = \frac{1}{\omega_n}\sqrt{\frac{A}{2}\tan^{-1}\frac{\omega_{if}^2}{\omega_n^2}} \tag{A7}$$

Expression (A7) is exact for the total RMS relative phase error if $S_\phi(\omega) = \frac{A}{\omega^3}$ in the region of interest. (However, the proper application of these results is predicated upon the PLL maintaining lock.)

APPENDIX B

APPROXIMATION OF THE INTEGRAL OF A DECISION VARIABLE

In the Analysis section, the decision variable q was used in the expression for the probability of error. This decision variable is the *sum* of two random components whose distribution must be determined. This appendix concerns the approximation

$$\frac{1}{T} \int_{0}^{T} \cos \phi(t)dt \simeq \cos \phi \qquad (B1)$$

which will physically be justified for the choice of parameters. The alternate approximation

$$\frac{1}{T} \int_{0}^{T} \cos \phi(t)dt \simeq \frac{1}{T} \int_{0}^{T} \left[1 - \frac{1}{2}\phi^2(t)\right]dt \qquad (B2)$$

is not advantageous in this case. (The subscript "in" again has been dropped from $\phi(t)$ for simplicity.)

The integral of a physically occurring random process, such as $\cos \phi(t)$, over definite limits of time, is a random variable (see appendix D). Thus in the approximation $\frac{1}{T} \int_{0}^{T} \cos \phi(t)dt \simeq \cos \phi$, the random variable $\frac{1}{T} \int_{0}^{T} \cos \phi(t)dt$ is replaced by the random variable $\cos \phi$ that is obtained from the random process $\cos \phi(t)$ by fixing the time $t = t_0$ (with $0 < t_0 \le T$).

Proceeding with the discussion of the quantity $\frac{1}{T} \int_{0}^{T} \cos \phi(t)dt$, consider the following hypothetical experiment. Suppose that a particular time function (realization) from the random process $\cos \phi(t)$ is the input to an averaging device that performs the operation $\frac{1}{T} \int_{0}^{T}$. Thus the output is $\frac{1}{T} \int_{0}^{T} \cos \phi(t)dt$, and the question arises, When is it nearly the same as the instantaneous value of the input? Clearly, the output will be almost the same as the input when the input does not change appreciably in the interval of time from 0 to T during which the device performs its averaging operation. Consequently, the relationship between the fluctuations that the input can undergo and the averaging time T needs to be examined. Since in reality T is the (telemetry) symbol period and it is fixed by the given bit rate $\frac{1}{T}$, it is preferable to study the changeability of the input. Furthermore, since the input $\cos \phi(t)$ to the hypothetical averaging device is a function of $\phi(t)$, it suffices to study the fluctuations that $\phi(t)$ can undergo. Thus the power spectral density S_ϕ that contains information about the frequency content of $\phi(t)$ will be studied.

In the analysis section, it was explained that the phase jitter process $\phi(t)$ in a phase lock loop receiver has the power spectral density

$$S_\phi(\omega) = \frac{A\omega}{\omega_n^4 + \omega^4} \qquad (B3)$$

over the frequency range of interest, and S_ϕ is negligible outside of this range. Since S_ϕ decreases as $1/\omega^3$ when ω increases, $\phi(t)$ does not contain any high frequencies within the significant range. This implies that $\cos \phi(t)$ varies only slowly so that its instantaneous value is close to the average value over a reasonably small interval of time. Defining the cutoff frequency f_c (in Hertz) as the frequency at which the value of the power spectral density S_ϕ is 3 dB below its maximum value, a quantitative relationship can be obtained between the length of time T over which the device averages the input and the frequency characteristics of $\phi(t)$. Since the averaging device gathers information about the input only during a T-second interval, an analogy to the Sampling Theorem for nonrandom signals may be drawn. According to this theorem, a time function containing no frequencies higher than f_c Hertz can be completely characterized by values of the function at instants of time separated by $1/2f_c$ seconds. Applying the theorem it becomes evident that the time function $\cos \phi(t)$ does not change much during the interval T seconds when $T < 1/2f_c$. Thus the output $\frac{1}{T} \int_0^T \cos \phi(t)dt$ from the device performing the operation $\frac{1}{T} \int_0^T$ will be almost the same as the input, $\cos \phi(t)$, for some fixed t between 0 and $T < 1/2f_c$. Since the time function $\cos \phi(t)$ does not fluctuate much during the T-second interval, it is clear that an arbitrary point t_0, with $0 < t_0 \leq T$, may be chosen to represent the average value $\frac{1}{T} \int_0^T \cos \phi(t)dt$ by the instantaneous value $\cos \phi(t_0)$ of the time function $\cos \phi(t)$. Writing $\cos \phi$ for $\cos \phi(t_0)$, the approximation

$$\frac{1}{T} \int_0^T \cos \phi(t)dt \simeq \cos \phi$$

is obtained when $T < 1/2f_c$ with f_c the 3 dB cut-off frequency of S_ϕ. This approximation will be useful in appendix E where the distribution of the decision variable q will be determined.

Now the disadvantages that arise from the alternate approximation will briefly be indicated (ref. 8, pp. 192-195)

$$\frac{1}{T} \int_0^T \cos \phi(t)dt \simeq \frac{1}{T} \int_0^T \left[1 - \frac{1}{2}\phi^2(t)\right]dt$$

$$\simeq 1 - \frac{1}{2T} \int_0^T \phi^2(t)dt$$

First the approximation, $\cos \phi(t) \simeq 1 - (1/2)\phi^2(t)$ when $\phi(t)$ is small, must be made; then one has to determine the distribution of the random variable $\frac{1}{2T}\int_0^T \phi^2(t)dt$. The distribution of this random variable has been only approximately found when (i) $\phi(t)$ is a normal process and (ii) for power spectra of the form $S_\phi(\omega) = 1/(a + \omega^2)$ and of the form $S_\phi(\omega) = $ constant for $-\omega_0 < \omega < \omega_0$, $S_\phi(\omega) = 0$ otherwise (refs. 9, 10). Since in this model the phase jitter process $\phi(t)$ is not of this type, rather $\phi(t)$ has Viterbi's distribution (as stated in the analysis section) and $S_\phi(\omega) = A\omega/(\omega_n^4 + \omega^4)$, the wealth of

existing knowledge does not help. Fortunately the physical situation
suggested a simpler approximation so that there was no need to use a number
of approximations that do not apply directly to the model.

APPENDIX C

DERIVATION OF THE PROBABILITY DENSITY FUNCTION OF $\cos \phi(t)$

In this appendix the probability density function g of the random variable $Z(t) \triangleq \cos \phi(t)$, at a fixed time t, is derived from the probability density function p of the random variable $\phi(t)$. Since $\phi(t)$ represents the phase jitter process, it was reasonable to assume in the analysis that its probability density function has Viterbi's form (ref. 3)

$$p(\phi) = \begin{cases} \dfrac{e^{\alpha \cos \phi}}{2\pi I_o(\alpha)} \, , & -\pi < \phi < \pi \\[2em] 0 \quad , & \text{otherwise} \end{cases} \tag{C1}$$

The real number ϕ stands for one value of the random process $\phi(t)$ at time t. Let z stand for the corresponding value of the transformed random process $Z(t) = \cos \phi(t)$ at the same time t.

Now the probability density function g(z) will be expressed in terms of the probability density function $p(\phi)$. Since z is the argument of the desired function g(z) and since the argument of the given function $p(\phi)$ is ϕ, first ϕ is obtained as a function of z so that $p(\phi)$ can be written in the form $p[\phi(z)]$. From $z = \cos \phi$ it follows that $\phi = \phi(z) = \cos^{-1}z$. Now for any given real number z_0 that lies between -1 and 1, the equation
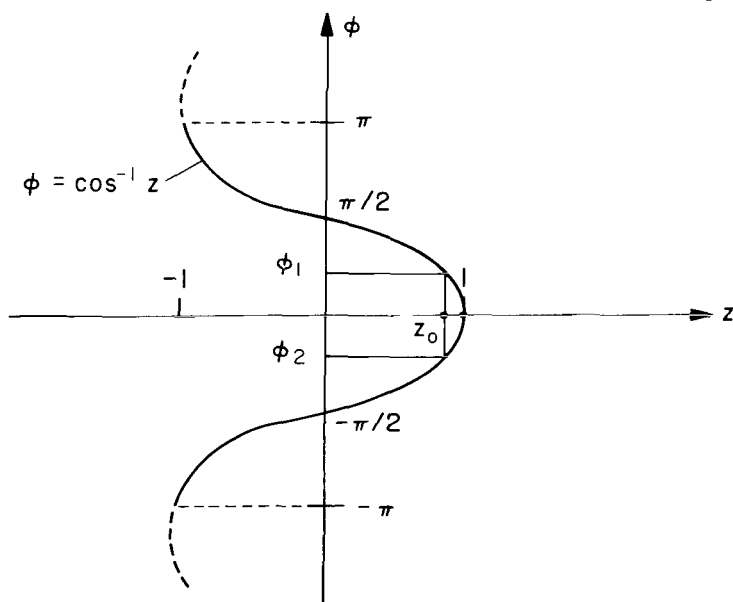
$$\phi = \cos^{-1}z_0 \tag{C2}$$

Figure 13.- The function $\cos^{-1}z$.

has two solutions, denoted by $\phi = \phi_1$ and $\phi = \phi_2$, which lie between $-\pi$ and π, as shown in figure 13 for one particular choice of z_0. This figure shows that the function $\cos^{-1}z$ is symmetrical with respect to the z-axis. This means that one of the solutions of the equation $\phi = \cos^{-1}z_0$ is the negative of the other solution; that is,

$$\phi_2 = -\phi_1$$

which will subsequently be used in the argument of the function $p(\phi)$.

The transformation $\cos \phi = z$ of the value ϕ (of the random variable $\phi(t)$ for fixed t) to the corresponding value z (of the new random variable Z) transforms the probability element $[p(\phi_1) + p(\phi_2)]d\phi$ to the corresponding probability element $g(z_0)dz$. In fact, the two probabilities are equal; that is,

$$g(z_0)dz = [p(\phi_1) + p(\phi_2)]d\phi \tag{C3}$$

because probability must be conserved under the transformation. This transformation of probability can be represented graphically as a transformation of area elements in figure 14. (Note that the sum of the areas of the shaded elements equals the area of the crosshatched element.)
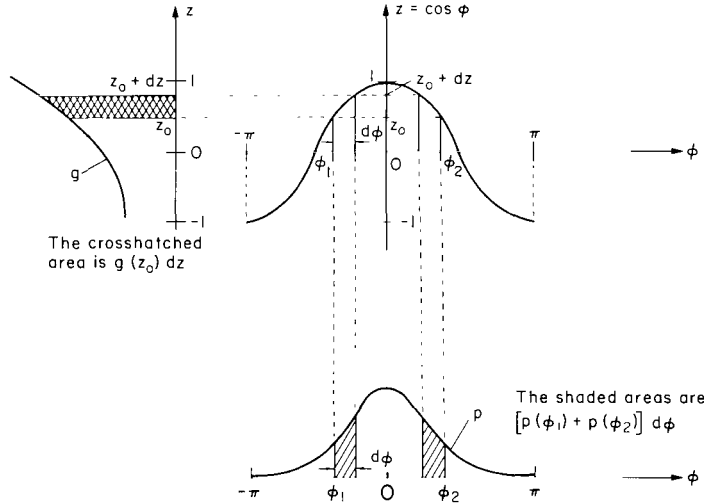

Figure 14.- The transformation of probabilities.

As can be seen in figure 14, the magnitude of the derivative $d\phi/dz = (d \cos^{-1}z)/dz$ at the point z_0 is the scale factor by which the shaded areas are transformed to the crosshatched area. From this geometrical reasoning, which is based on the principle of conservation of probability, the general relationship follows

$$g(z) = \left|\frac{d\phi}{dz}\right| [p(\phi_1) + p(\phi_2)] \tag{C4}$$

31

which expresses the transformation of probabilities under the transformation $\cos \phi = Z$ of random variables. Computing

$$\left|\frac{d\phi}{dz}\right| = \left|\frac{d \cos^{-1}z}{dz}\right|$$

$$= \frac{1}{\sqrt{1 - z^2}} \qquad z \neq \pm 1 \qquad\qquad (C5)$$

and realizing that p is an even function, that is,

$$p(\phi_1) = p(-\phi_2)$$

$$= p(\phi_2)$$

(because $\phi_2 = -\phi_1$), the formula

$$g(z) = \left|\frac{d\phi}{dz}\right| 2p(\phi)$$

$$= \frac{1}{\pi I_0(\alpha)} \frac{e^{\alpha z}}{\sqrt{1 - z^2}} \qquad\qquad (C6)$$

is obtained. The variable ϕ is restricted to the interval $-\pi < \phi < \pi$, and $z = \cos \phi$ is restricted to the interval $-1 < z < 1$. When either $z < -1$ or $z > 1$, there are no values of ϕ corresponding to these values of z. Thus the probability that either the random variable $Z < -1$ or $Z > 1$ is 0.

This completes the proof that the random variable $Z \triangleq \cos \phi$ has the probability density function

$$g(z) = \begin{cases} \dfrac{1}{\pi I_0(\alpha)} \dfrac{e^{\alpha z}}{\sqrt{1 - z^2}}, & -1 < z < 1 \\ \\ 0, & \text{otherwise} \end{cases}$$

Figures 15 and 16 show this probability density function for various values of the parameter $\sigma_\phi \overset{\triangle}{=} 1/\sqrt{\alpha}$, and figure 15 also shows the transformation of $p(\phi)$ to $g(z)$.
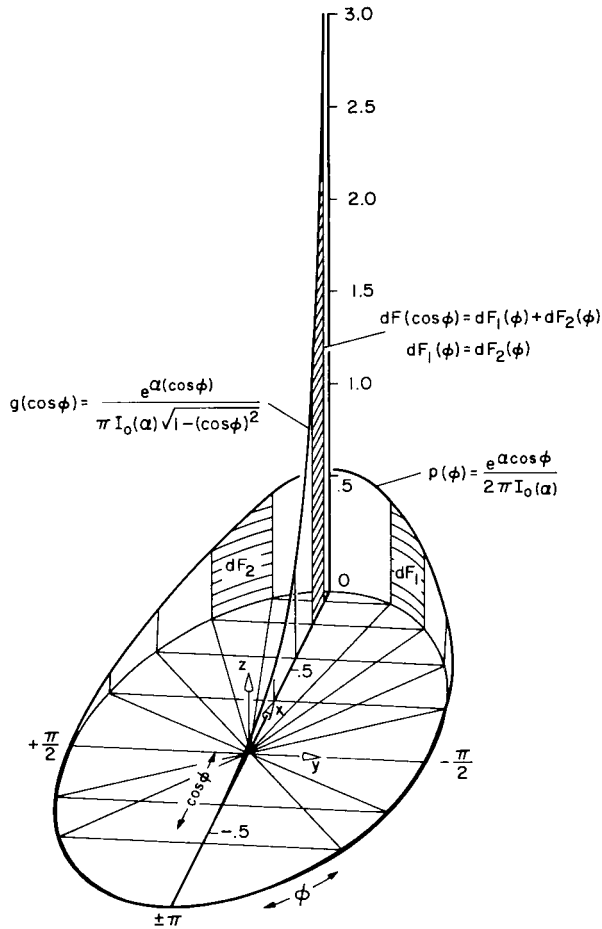

$dF(\cos\phi) = dF_1(\phi) + dF_2(\phi)$

$dF_1(\phi) = dF_2(\phi)$

$g(\cos\phi) = \dfrac{e^{\alpha(\cos\phi)}}{\pi I_0(\alpha)\sqrt{1-(\cos\phi)^2}}$

$p(\phi) = \dfrac{e^{\alpha\cos\phi}}{2\pi I_0(\alpha)}$

Figure 15.- Transformation of PDF under the change of variables from "ϕ" to "$\cos\phi$." The PDF's are drawn to scale for $\sigma_\phi = 0.56$, $\alpha = 0.312$ $(\alpha = 1/\sigma_\phi^2)$; $p(\phi)$ is on the cylinder of unit radius, perpendicular to the x-y plane; ϕ is on the unit circle; $g(\cos\phi)$ is in the x-z plane; $\cos\phi$ is on the x-axis; dF denotes elements of probability.
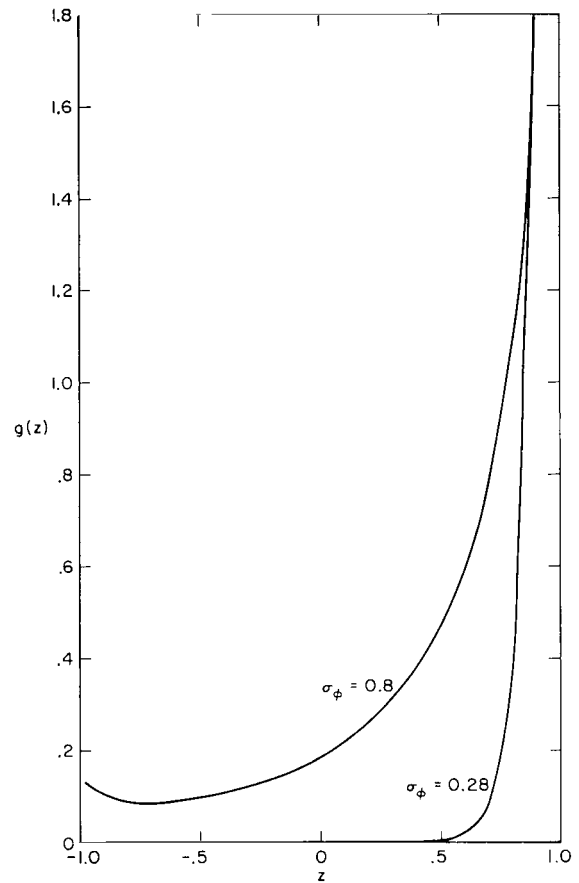

Figure 16.- Probability density function; $g(z) = e^{\alpha z}/\pi I(\alpha)(1 - z^2)^{1/2}$, $\alpha = 1/\sigma_\phi^2$, for two values of σ_ϕ.

33

DERIVATION OF THE PROBABILITY DENSITY FUNCTION OF $\frac{1}{KT} \int_o^T n(t)dt$

The decision variable q was used in the expression for the probability of error associated with a telemetry signal. This decision variable is the sum of two random components. The first random component $\frac{1}{T} \int_o^T \cos \phi(t)dt$ was treated in appendixes B and C. The second random component $\frac{1}{KT} \int_o^T n(t)dt$, where K is a real constant, will be discussed here.

It will be necessary first to give a physical meaning to the quantity $\frac{1}{T} \int_o^T n(t)dt$. The random process n(t) consists of a collection of deterministic time functions (realizations) that can be represented in the set $\{n_1(t), n_2(t), \ldots, n_i(t), \ldots, n_k(t), \ldots \}$. In any one particular experiment, one time function, $n_i(t)$ is integrated over an interval of T seconds yielding the number $\int_o^T n_i(t)dt$. Then this number is divided by the integration time T giving the number $\frac{1}{T} \int_o^T n_i(t)dt$ which is recognized as the time average of the function $n_i(t)$ over the interval of T seconds. When this experiment is repeated, a different time function, $n_k(t)$ is involved whose time average $\frac{1}{T} \int_o^T n_k(t)dt$ is computed. Continuing the experiments in this manner, a collection of time averages is obtained which may be represented in the set $\left\{\frac{1}{T} \int_o^T n_1(t)dt, \frac{1}{T} \int_o^T n_2(t)dt, \ldots, \frac{1}{T} \int_o^T n_i(t)dt, \ldots, \frac{1}{T} \int_o^T n_k(t)dt, \ldots \right\}$. The elements of this set are real numbers that resulted from having performed the experiments 1, 2, . . . , i, . . . , k, ... Before each of these experiments it was not known which one of the time function averages would be computed. Consequently, it was also not known which one of the elements in the above set would be the outcome of the particular experiment. This ignorance renders the set above a random collection, and it is represented by the symbol $\frac{1}{T} \int_o^T n(t)dt$ that is called a random variable in probability theory. Thus, for any random process such as n(t), from which the integral over a constant interval T of time is computed, such as $\int_o^T n(t)dt$, a random variable is obtained. Figure 17 summarizes graphically these introductory remarks. The sum of the shaded areas above the t-axis minus the sum of the crosshatched areas below the t-axis represents T times the time average of the respective time function. Figure 17 is drawn for an arbitrary random process n(t); in the following discussion n(t) will stand for a white, Gaussian noise process.

Now some qualitative statements follow about the random variable

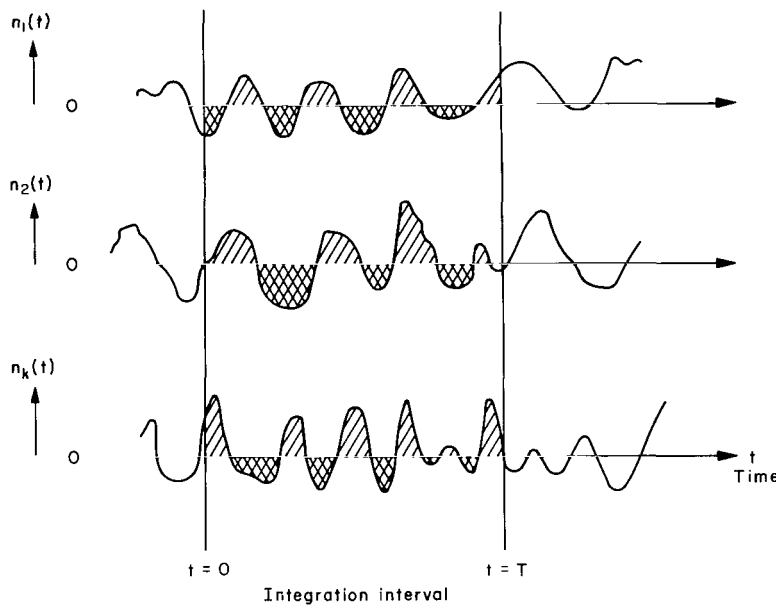$$Y \triangleq \frac{1}{KT} \int_o^T n(t)dt$$

Figure 17.- Typical time functions from the random process n(t).

In the analysis it was assumed that the noise process n(t) obeys the normal probability law with zero mean and variance σ^2 so that the probability density function of n(t) is

$$h(n) = \frac{1}{\sigma\sqrt{2\pi}} \, e^{\frac{-n^2}{2\sigma^2}}$$

for $-\infty < n < \infty$. This means that the noise process n(t) takes a value n_k in the interval from a to a + dn with probability

$$h(n_k)\,dn = \frac{1}{\sigma\sqrt{2\pi}} \, e^{\frac{-n_k^2}{2\sigma^2}} \, dn$$

When the value n_k approaches infinity, the probability $\lim_{n_k \to \infty} h(n_k)dn$ of this happening tends to 0 at the rate $e^{-n_k^2}$. Thus it follows that the integral $\int_0^T n(t)dt$ exists and converges for almost all time functions in the set $\{n_1(t), n_2(t), \ldots\} = n(t)$. Davenport and Root (ref. 11) show that under these conditions the integral of a normal random process is itself normally distributed. Since a normal random variable is statistically completely specified by giving its mean and variance, it is necessary to determine only those parameters in order to write its probability density function.

The following is the determination of the mean E{Y}, and the variance σ_Y^2 of the random variable

$$Y \triangleq \frac{1}{KT} \int_0^T n(t)dt$$

that represents 1/K times the time average of the random process n(t) over the interval of length T seconds. Since the expectation E is linear

$$E\{Y\} = E\left\{\frac{1}{KT} \int_O^T n(t)dt\right\}$$

$$= \frac{1}{KT} \int_O^T E\{n(t)\}dt$$

Since the mean $E\{n(t)\}$ of the noise process $n(t)$ was assumed to be 0, it follows that

$$E\{Y\} = 0$$

In such a case the variance $\sigma_Y^2 \triangleq E\{[Y - E\{Y\}]^2\}$ reduces to the mean square value $E\{Y^2\}$ which will be computed next:

$$E\{Y^2\} = E\left\{\left(\frac{1}{KT} \int_O^T n(t)dt\right)^2\right\}$$

$$= \frac{1}{(KT)^2} E\left\{\int_O^T \int_O^T n(t)n(u)dt\ du\right\}$$

Since the double integral in the second equation above can be regarded as the limit of a double sum, and since a double sum is simply one large sum, the linearity of the expectation E allows us to interchange the order of expectation and integration. Thus

$$E\left\{\int_O^T \int_O^T n(t)n(u)dt\ du\right\} = \int_O^T \int_O^T E\{n(t)n(u)\}dt\ du$$

$$= \int_O^T \int_O^T R_n(t,u)dt\ du$$

where R_n is the autocorrelation function of the noise process $n(t)$ which is also assumed to be stationary so that $R_n(t,u) = R_n(t-u)$. Since $S_n(f) = (N_O/2)$ W/Hz for $-\infty < f < \infty$, it follows from the Wiener-Khintchine Theorem[1] that

$$R_n(t - u) = \mathfrak{F}^{-1}\{S_n(f)\}$$

$$= \frac{N_O}{2} \delta(t - u) \text{ watts}$$

---

[1]The Wiener-Khintchine Theorem states that the autocorrelation function and power spectral density of a wide sense stationary process are a Fourier transform pair.

where the symbol $\mathfrak{F}^{-1}$ denotes the inverse Fourier transformation. Using one of the properties of the Dirac delta function, that is,

$$\int \delta(w)dw = 1$$

and with the limits on the integral suitably chosen, the following equations can be written:

$$\int_0^T \int_0^T R_n(t - u)dt\,du = \int_0^T \int_0^T \frac{N_0}{2} \delta(t - u)dt\,du$$

$$= \frac{N_0}{2} \int_0^T du$$

$$= \frac{N_0 T}{2}$$

Thus the mean square value

$$E\{Y^2\} = \frac{N_0}{2K^2T}$$

is obtained which equals the variance σ_Y^2 of the random variable

$$Y = \frac{1}{KT} \int_0^T n(t)dt$$

The probability density function of Y then is

$$h(y) = \frac{1}{\sqrt{(N_0/2K^2T)}\sqrt{2\pi}} e^{\frac{-y^2}{2(N_0/2K^2T)}}$$

for $-\infty < y < \infty$. This completes the determination of the probability density function of the random variable $\frac{1}{KT} \int_0^T n(t)dt$, taking real values y, that is the second random component in the decision variable q.

EVALUATION OF SYMBOL ERROR PROBABILITY

In the analysis the expression

$$P_e = \int_{-\infty}^{0} p_q(x)\,dx \tag{E1}$$

represented the probability of error where p_q is the probability density function of the decision variable q. Since the random variable q is the sum of two independent random variables with probability density functions h and g, respectively, it follows from the Convolution Theorem[1] that

$$p_q(x) = h(x) * g(x)$$

$$= \int_{u_1}^{u_2} h(x - u)g(u)\,du \tag{E2}$$

In appendix D the probability density function

$$h(x) = \frac{1}{\sqrt{(N_0/2K^2T)}\,\sqrt{2\pi}}\, e^{\frac{-x^2}{2(N_0/2K^2T)}}, \qquad -\infty < x < \infty \tag{E3}$$

and in appendix C the probability density function

$$g(x) = \begin{cases} \dfrac{e^{\alpha x}}{\pi I_0(\alpha)\,\sqrt{1 - x^2}}, & -1 < x < 1 \\[2ex] 0, & \text{otherwise} \end{cases} \tag{E4}$$

were derived. Since the function $g(u)$ in the integrand of (E2) is zero for values of the argument u that are outside of the interval from -1 to 1 and since the argument $x - u$ of h is unrestricted, the range of integration has only to extend from $u_1 = -1$ to $u_2 = 1$. (This observation can be proved rigorously by the method outlined in the article cited in the footnote.)

---

[1]The concept of convolution and its physical meaning are lucidly presented in the article by T. J. Healy, reference 12.

Substituting the integral for p_q into the expression for the probability of error (E1) results in

$$P_e = \int_{-\infty}^{0} \left[\int_{-1}^{1} h(x - u)g(u)du \right] dx \qquad (E5)$$

Now P_e will be expressed in terms of tabulated functions. Since the integrand $h(x - u)g(u)$ is (absolutely) continuous for $-1 < u < 1$ and $-\infty < x < 0$, the order of integration may be interchanged so that

$$P_e = \int_{-1}^{1} \left[\int_{-\infty}^{0} h(x - u)dx \right] g(u)du \qquad (E6)$$

Now define

$$v \triangleq - \frac{x - u}{\sqrt{2(N_O/2K^2T)}}$$

where u is fixed, so that

$$dx = - \sqrt{2(N_O/2K^2T)} \, dv$$

The limits of integration $x = -\infty$ and $x = 0$ become $v = +\infty$ and

$$v = \frac{u}{2(N_O/2K^2T)} \triangleq v_\ell$$

Then the integral in brackets of (E6) is written

$$\int_{-\infty}^{0} h(x - u)dx = \frac{1}{\sqrt{\pi}} \int_{v_\ell}^{\infty} e^{-v^2} \, dv \qquad (E7)$$

having used the formula

$$-\int_{b}^{a} f(y)dy = \int_{a}^{b} f(y)dy$$

The co-error function, erfc, is defined by (ref. 4, entry 7.1.2)

$$\text{erfc}(v_\ell) \triangleq \frac{2}{\sqrt{\pi}} \int_{v_\ell}^{\infty} e^{-v^2} \, dv$$

39

so that

$$\frac{1}{\sqrt{\pi}} \int_{v_\ell}^{\infty} e^{-v^2} \, dv = \frac{1}{2} \, \text{erfc}(v_\ell)$$

The final expression for the probability of error is

$$P_e = \frac{1}{2} \int_{-1}^{1} \text{erfc}\left[\frac{u}{\sqrt{2(N_o/2K^2T)}}\right] g(u)\,du \qquad \text{(E8)}$$

where

$$g(u) = \begin{cases} \dfrac{e^{\alpha u}}{\pi I_o(\alpha)\sqrt{1 - u^2}}, & -1 < u < 1 \\[2ex] 0, & \text{otherwise} \end{cases}$$

and

$$I_o(\alpha) \overset{\Delta}{=} \frac{1}{\pi} \int_o^{\pi} e^{\alpha \cos \phi} \, d\phi$$

is the modified Bessel function of order zero (ref. 4, entry 9.6.19). Also,

$$\alpha = \frac{1}{E\{\phi_{in}^2\}} \simeq \frac{1}{\phi_{in}^2} \text{ or } \frac{1}{\sigma_\phi^2}$$

since the mean of ϕ_{in} is zero.

The final question concerns the form that the expression for P_e assumes under strong signal conditions. Under such conditions the random variable $Y = \frac{1}{KT} \int_o^T n(t)dt$ is much more likely to take on small values than large. Since $\sigma_Y^2 = N_o/2K^2T$ the variance of Y (or the noise-to-signal ratio), a strong signal condition is then equivalent to the requirement that σ_Y^2 become vanishingly small. In such case the probability density $h(y)$ of Y will be large about its mean $E\{Y\} = 0$ and will decrease rapidly for values y away from the mean. In the limit as σ_Y^2 approaches 0, all probability is concentrated at the mean, that is,

$$\lim_{\sigma_Y \to 0} h(y) = \lim_{\sigma_Y \to 0} \frac{1}{\sigma_Y \sqrt{2\pi}} e^{-\frac{y^2}{2\sigma_Y^2}}$$

$$= \delta(y)$$

From the sifting property

$$\int_{-b}^{b} \delta(x - u) g(u) du = g(x)$$

it follows that

$$p_q(x) = h(x)*g(x) = g(x)$$

when $\sigma \to 0$. Thus

$$P_e = \int_{-\infty}^{0} g(x) dx = \int_{-1}^{0} g(x) dx$$

because $g(x) = 0$ for $x < -1$. Substitution of the probability density function g yields the expression

$$P_e = \frac{1}{\pi I_0(\alpha)} \int_{-1}^{0} \frac{e^{\alpha x}}{\sqrt{1 - x^2}} dx$$

for the probability of error under strong signal conditions. In this case P_e equals the probability of $\cos \phi$ taking negative values which is a function of the variance. Evaluation by computer showed that the previous expression for P_e (containing the co-error function erfc) yields the same values for P_e when σ_γ is small as does the preceding expression. Figure 8 shows P_e as a function of the standard deviation of ϕ_{in} and as a function of $\frac{1}{2(N_0/2K^2T)} \triangleq \frac{ST}{N_0}$ (expressed in dB).

REFERENCES

1. Baghdady, E. J.; and Lippincott, S.: Characterization of Causes of Signal Phase and Frequency Instability. Final Report (contract NAS2-5337), NASA CR-73442, 1970.

2. Salwen, H. C.: Study of Pioneer Spacecraft Oscillator Stability. Final Report (contract NAS2-5021), NASA CR-73307, 1968.

3. Viterbi, A. J.: Principles of Coherent Communication. McGraw-Hill Book Co., N. Y., 1966.

4. Abramowitz, Milton; and Stegum, Irene A., eds.: Handbook of Mathematical Functions with Formulas, Graphs and Mathematical Tables. National Bureau of Standards, Appl. Math. Ser. 55, June 1964.

5. Gardner, F. M.: Phaselock Techniques. John Wiley and Sons Inc., N. Y. 1966.

6. Baghdady, E. J.: Lectures on Communication System Theory. McGraw-Hill Book Co., N. Y., 1961.

7. Anon.: Standard Mathematical Tables, 13th Edition, Chemical Rubber Co., 1964, eq. #44.

8. Blake, I. F.; and Lindsey, W. C.: Communications Systems Development: Effects of Phase-Locked Loop Dynamics on Phase-Coherent Communications. JPL Space Programs Summary, 37-54, vol. III, Dec. 31, 1968, pp. 192-195.

9. Grenander, U.; Pollak, H. O.; and Slepian, D.: The Distribution of Quadratic Forms in Normal Variates. J. Soc. Indust. Appl. Math., vol. 7, Dec. 1959, pp. 374-401.

10. Schwartz, M. I.: Distribution of the Time-Average Power of a Gaussian Process. IEEE Trans. Info. Th., vol. IT-16, no. 1, Jan. 1970, pp. 17-26.

11. Davenport, W. B., Jr.; and Root, W. L.: An Introduction to the Theory of Random Signals and Noise. McGraw-Hill Book Co., N. Y., 1958.

12. Healy, T. J.: Convolution Revisited. IEEE Spectrum, vol. 6, no. 4, April 1969, pp. 87-93.

"*The aeronautical and space activities of the United States shall be conducted so as to contribute . . . to the expansion of human knowledge of phenomena in the atmosphere and space. The Administration shall provide for the widest practicable and appropriate dissemination of information concerning its activities and the results thereof.*"

— NATIONAL AERONAUTICS AND SPACE ACT OF 1958

NASA SCIENTIFIC AND TECHNICAL PUBLICATIONS

TECHNICAL REPORTS: Scientific and technical information considered important, complete, and a lasting contribution to existing knowledge.

TECHNICAL NOTES: Information less broad in scope but nevertheless of importance as a contribution to existing knowledge.

TECHNICAL MEMORANDUMS: Information receiving limited distribution because of preliminary data, security classification, or other reasons.

CONTRACTOR REPORTS: Scientific and technical information generated under a NASA contract or grant and considered an important contribution to existing knowledge.

TECHNICAL TRANSLATIONS: Information published in a foreign language considered to merit NASA distribution in English.

SPECIAL PUBLICATIONS: Information derived from or of value to NASA activities. Publications include conference proceedings, monographs, data compilations, handbooks, sourcebooks, and special bibliographies.

TECHNOLOGY UTILIZATION PUBLICATIONS: Information on technology used by NASA that may be of particular interest in commercial and other non-aerospace applications. Publications include Tech Briefs, Technology Utilization Reports and Technology Surveys.

Details on the availability of these publications may be obtained from:

SCIENTIFIC AND TECHNICAL INFORMATION OFFICE

NATIONAL AERONAUTICS AND SPACE ADMINISTRATION
Washington, D.C. 20546